

*Human systemic and intestinal IgA responses
against the mucinase YghJ following
experimental infection with
enterotoxigenic Escherichia coli*

Saman Riaz



Centre for International Health, Department of Global Health & Primary Care

Faculty of Medicine

University of Bergen

May 2021

Mphil. Candidate:

Saman Riaz

Centre for International Health, Department of Global Public Health and Primary Care

Department of Clinical Sciences (K2)

Faculty of Medicine

University of Bergen, Norway

saman.riaz@student.uib.no

Main Supervisor:

Kurt Hanevik, MD, PhD

Associate Professor / Infectious diseases specialist

Department of Clinical Science (K2), Faculty of Medicine, University of Bergen, Norway

Norwegian National Advisory Unit for Tropical Infectious Diseases, Medical Department,

Haukeland University Hospital, Bergen, Norway.

kurt.hanevik@uib.no

Co-supervisor:

Hans Steinsland, PhD

Researcher

CISMACH, Centre for International Health, Department of Global Public Health and Primary Care

Faculty of Medicine

University of Bergen, Norway

hans.steinsland@uib.no

International collaborators:

1. Anders Boysen, GlyProVac ApS and Department of Biochemistry and Molecular Biology, University of Southern Denmark

2. Ann Zahle Anderson, GlyProVac ApS, Odense, Denmark

*Human systemic and intestinal IgA responses
against the mucinase YghJ following
experimental infection with
enterotoxigenic Escherichia coli*

Saman Riaz



This thesis is submitted in partial fulfilment of the requirements for the degree of
Master of Philosophy in International Health at the University of Bergen.

Centre for International Health, Department of Global Health and Primary care,
Faculty of Medicine, University of Bergen, Norway

May 2021

TABLE OF CONTENTS

1. INTRODUCTION	9
1.1. Enterotoxigenic <i>Escherichia coli</i>	9
1.2. Immune responses to non-invasive gut pathogens.....	12
1.2.1. Innate and adaptive immunity.....	12
1.2.1.1. Innate immunity	12
1.2.1.2. Adaptive immunity	12
1.2.2. IgA in the gut.....	14
1.2.3. The process of transcytosis.....	15
1.2.4. Secretory immunoglobulin A (SIgA)	15
1.2.5. Other immunoglobulins in the gut.....	16
1.2.6. Immune response to glycosylated antigens.....	16
2. RATIONALE.....	17
3. MATERIALS, METHODS, AND METHODOLOGICAL CONSIDERATIONS.....	21
3.1. Brief description of the experimental ETEC infection study.....	21
3.2. Experimental infection of the volunteers	21
3.3. Infecting strain	22
3.4. Sampling methods	22
3.5. Materials	24
3.5.1. Equipment.....	24
3.5.2. Reagents	25
3.5.3. Buffers.....	26
3.5.4. Flow cytometer	27
3.5.4.1. Flow Cytometer settings and fluorochromes	27
3.6. Methods.....	29
3.6.1. Preparation of lavage samples.....	29
3.6.2. Antigen production	29
3.6.3. Quantitation of proteins	29
3.6.4. Covalently coupling YghJ to beads	30
3.6.5. Flow cytometric bead immunoassay	34
3.6.6. Total IgA quantitation	35
3.6.7. Specificity Assay.....	37
3.6.8. Gating strategy.....	38
3.6.8.1. Gating strategy for YghJ-specific IgA in lavage and serum samples	38
3.6.8.2. Gating strategy for Total IgA in lavage samples in FlowJo.....	39
3.6.9. Data generation and analyses.....	40
3.6.9.1. Standard curve for lavage and serum samples.....	40
3.6.9.2. Normalization of IgA levels in lavage specimens.....	41
3.6.9.3. Lavage and serum samples fold change calculations	41

3.6.9.4. Lavage and serum specificity assay calculations	42
3.6.9.5. Statistical Analysis	43
4. DISCUSSION	44
4.1. Methodological Aspects.....	44
4.1.1. Coupling of beads	44
4.1.2. Testing effects of multiplexing beads	46
4.1.3. Testing varying assay salinity	47
4.1.4. Optimal dilution of samples.....	47
4.1.5. Specificity assay optimization	48
4.1.6. Bead stability.....	50
4.1.7. Other considerations	51
4.2. Strengths of the study.....	51
4.3. Limitations of the study	52
4.4. Conclusions	53
4.5. Future Aspects	54
REFERENCES	55
APPENDIX.....	59
A. Guidelines from the journal	59
B. Ethical approval	59

I. ACKNOWLEDGEMENTS

In the name of Allah , the most Gracious, the most Merciful

I would like to thank **Kurt Hanevik**, my main supervisor, for showing me the path and guiding me through it. His attributes of kindness, patience, constant encouragement, mindfulness, and generosity with his time aided my amateurishness in the field. I have immense regard for his efforts and his time that not only helped me in my work but also helped me grow as a person.

I would extend my gratitude to my co-supervisor **Hans Steinsland** for his positivism, kindness, practical opinions, and exceptional attitude to trouble shoot problems. And to **Oda Vedøy**, for being a constant voice in my head while working in the lab, for she taught me the basic workings there, and listening to the occasional vent outs.

Thanks to **Helene, Brith, Sonya, Marianne, Tove**, and others for being very helpful and making the environment at the '5th floor' pleasant and friendly. **Linda Karen** from Centre for International Health has always been very kind and carried a magic wand to solve all problems.

I would like to thank my parents (**Syed Riaz** and **Tahira**) and siblings (**Tayyaba, Ayesha, Bushra, Mariam, Abbas**) for all the support they have provided me with. I am appreciative of my friends **Mona** and **Linn** for being there, always. And to my beloved husband **Qamar**, for believing in me, and for listening to every ounce of progress or failure throughout the way.

In the end I would like to thank my daughters, the source of my pride, **Ayeza** and **Minha**, who always kept it down while I was reading. Without their patience and understanding, it would have been difficult. This is dedicated to them.

II. List of abbreviations

AIEC	Adherent-invasive <i>Escherichia coli</i>
ALS	Antibody in lymphocyte supernatant
AU	Arbitrary unit
BSA	Bovine serum albumin
CBA	Cytometric bead array
CF	Colonization factor
CFA/I	Colonization factor 1
CHIM	Controlled human infection model
CS	Coli surface antigen
DAEC	Diffusely adherent <i>Escherichia coli</i>
DALY	Disability adjusted life year
EAEC	Enteroaggregative <i>Escherichia coli</i>
EDC	N-(3-dimethylaminopropyl)-N'-ethyl carbodiimide HCl
EE	Environmental enteropathy
EHEC	Enterohemorrhagic <i>Escherichia coli</i>
EIEC	Enteroinvasive <i>Escherichia coli</i>
ELISA	Enzyme-linked immunosorbent assay
EPEC	Enteropathogenic <i>Escherichia coli</i>
ETEC	Enterotoxigenic <i>Escherichia coli</i>
FACS	Florescent-activated cell sorting
FSC-A	Forward scatter area
GALT	Gut-associated lymphoid tissue
gYghJ	Glycosylated YghJ
IgA	Immunoglobulin A
IgG	Immunoglobulin G
IgM	Immunoglobulin M
ILF	Isolated lymphoid follicle
LMICs	Lower-Middle income countries
LPS	Lipopolysaccharide
LT	Labile toxin

MES	(2-(N-morpholino) ethanesulfonic acid sodium salt)
MFI	Median fluorescence intensity
nYghJ	Non-glycosylated YghJ
PBS	Phosphate Buffer Saline
PE	Phycoerythrin
PEG	Poly (ethylene glycol) 2-aminoethyl ether acetic acid
pIgR	Polymeric immunoglobulin receptor
PTM	Post-translational modification
SC	Secretory component
SIgA	Secretory immunoglobulin A
SSC-A	Side scatter area
SlE	Secreted and surface-associated lipoprotein from <i>Escherichia coli</i>
ST	Stable toxin
STEC	Shiga toxin-producing <i>Escherichia coli</i>
Sulfo-NHS	N-(3-dimethylaminopropyl)-N'-ethyl carbodiimide HCl sodium N-hydroxysulfosuccinimide
T2SS	Type II Secretion system
Tris-HCl	Tris Hydrochloride
WC	Whole cell
WH	World Health Organization
WR	Working reagent

1. INTRODUCTION

1.1. Enterotoxigenic *Escherichia coli*

Escherichia coli (*E. coli*) is a bacteria often found in the gut of humans and most animals, with a number of pathogenic subtypes causing disease in an intestinal and extra-intestinal environment (2). *E. coli* bacteria are gram-negative, rod-shaped facultative anaerobes that can be classified into three major groups based on clinical benchmarks: commensal strains, intestinal pathogenic strains, and extraintestinal pathogenic strains (3, 4). Among intestinal pathotypes of *E. coli*, which are almost always transmitted through the faecal-oral route, seven pathotypes have been identified to date. They include adherent-invasive (AIEC), enteropathogenic (EPEC), enteroaggregative (EAEC), enterohemorrhagic or Shiga toxin-producing (EHEC/STEC), enteroinvasive (EIEC), diffusely adherent (DAEC), and enterotoxigenic *E. coli* (ETEC). ETEC is a non-invasive pathogen and causes diarrhoea due to the elaboration of toxins (3-5).

ETEC came to light as a distinct pathotype in the early 1970s when their pathogenesis of non-invasive, enterotoxin-mediated diarrhoea was identified, separating them from *Vibrio cholera* (6). ETEC usually spread through the faecal-oral route and proliferates in the small intestine. They usually possess a wide array of virulence factors that are implicated in the pathogenesis and that are therefore also often considered for use as antigens in vaccines against ETEC.

These ETEC antigens can be broadly classified into classical and non-classical antigens or novel antigens. Classical antigens include the lipopolysaccharides (LPS), colonization factors (CFs), heat-stable toxin (ST), and heat-labile toxin (LT) that have been extensively described; non-

classical antigens, on the other hand, have recently come to light as a result of further exploration of the extensive repertoire of virulence factors that these pathogens may produce.

ETEC, and most other *E. coli*, express O antigens, which are the outer domain of the LPS molecule. This category of antigens has the largest variability and elicits both adaptive and innate immune responses (7, 8).

ETEC can colonize parts of the small intestine through the production of CFs, which are the primary adhesion proteins (9). Approximately 25 different types have been associated with human ETEC. The colonization factors most commonly associated with ETEC diarrhoea include the Colonization Factor Antigen I (CFA/I), and the Coli Surface (CS) antigens 1 (CS1) to CS6. These are also known as the major colonization factors (10-12).

Once colonized, ETEC that infect humans produce either one or both of ST and LT. ST is small and nonimmunogenic, while LT is larger and elicits an immune response (13, 14). ST is also found in two close-to-identical variants called human (STh) and porcine (STp) ST. The production of toxins by ETEC plays a key role in the development of diarrhea. In children under 5 years of age from low- and middle-income countries (LMICs), infection with ST-producing ETEC, in particular those that produce STh, is more associated with moderate and severe diarrhoea, and an increased risk of death (15).

The epithelial cells in the intestines are covered by a thick layer of mucus that prevents the entry of bacteria. It is important for the pathogens to subvert this barrier to gain access to the receptors on the epithelial cells and establish colonization. For this purpose, many *E. coli*, including close to all of the most pathogenic ETEC, produce a highly conserved, large (~170 kDa), mucin degrading

metalloprotease called YghJ. It is also referred to as Secreted and surface-associated lipoprotein from *E. coli* (SsIE) (16). Compared to the commensal *E. coli*, ETEC secretes YghJ in plenitude. It degrades the major mucins, MUC2 and MUC3, in the small intestines in a dose-dependent manner (17). It is found in association with outer membrane vesicles of ETEC and relies on the type II secretion system (T2SS) for its secretion, which, in ETEC, is also used for secreting LT. YghJ is actively involved in the increased delivery of LT toxin to the epithelial cells, thus playing a significant role in the pathogenesis of ETEC (17, 18). YghJ is one of the non-classical antigens inciting an immune response during an ETEC infection (15, 19), making it a vaccine target that could help to induce a broadly protective immune response (20). In its native form, YghJ is a glycosylated antigen (21).

Glycosylation is part of the post-translational modification (PTM) of proteins, performed in both prokaryotic and eukaryotic cells. It is a multistep process resulting in the attachment of sugar moieties to the proteins that can influence the folding and stability of proteins and their biological functions (22).

Glycosylation of bacterial proteins is important in facilitating adhesion, colonization, and invasion of the host cells. It is associated with cellular core processes, antigenic variation, proteolytic and thermal stability of bacterial proteins, and protective immunity (21, 23, 24). Among *E. coli*, ETEC strains glycosylate their proteins more than the non-pathogenic strains, indicating a crucial role in the pathophysiology of the bacteria (21).

1.2. Immune responses to non-invasive gut pathogens

1.2.1. Innate and adaptive immunity

The gut is a dynamic environment with constant exposure to food particles, commensals, and other foreign antigens. Gut homeostasis is attained through an intricate balance between innate and adaptive immunity, that leads to tolerance towards commensals and eradication of pathogens (25).

1.2.1.1. Innate immunity

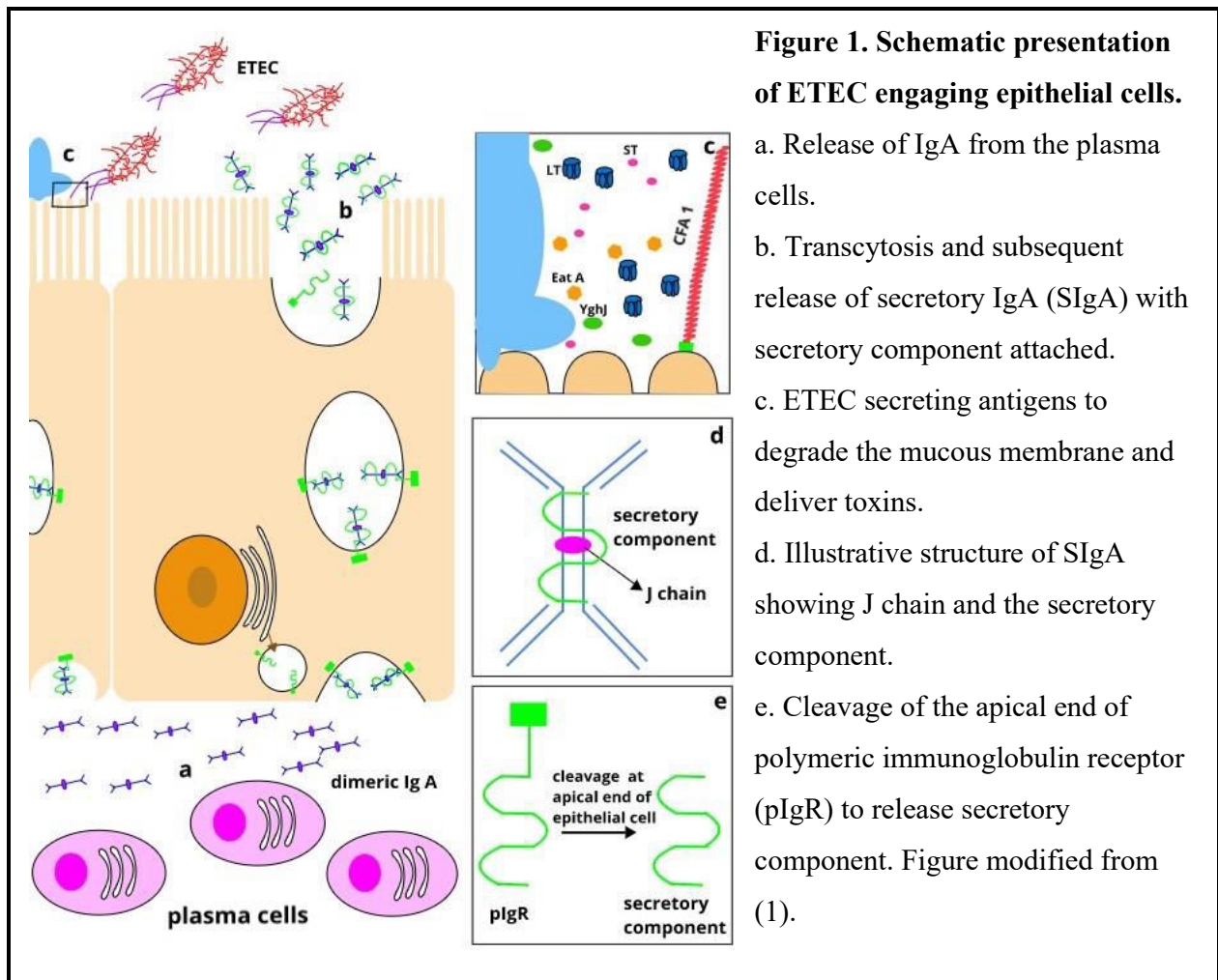
Innate immunity of the gut is the first line of defence against a potentially hostile environment produced by an enormous load of commensal bacteria, food particles, and external pathogens. Innate immunity is usually facilitated through epithelial cell linings, tight intercellular junctions, secretion of a thick layer of mucus, and production of anti-microbial molecules in the lamina propria. Dendritic cells, macrophages, and natural killer cells also play a role in the recognition of microbes and facilitate adaptive immunity. Together, they impede the invasion of microbes and limit the number of commensals in the gut (26). Since the gastrointestinal (GI) tract is burdened with a huge number of microorganisms, it does not appear logical that recognition of microorganisms by innate immunity will lead to an explicit, organism-specific inflammation and the effects of this inflammation.

1.2.1.2. Adaptive immunity

Adaptive immunity of the gut is mainly implemented by T-cells, B-cells, a subepithelial collection of lymphoid tissue known as gut-associated lymphoid tissues (GALT), and by isolated lymphoid follicles (ILFs) (27-29). Post-infection, B-cells located in the mucosa are activated in regional mucosa-associated lymphoid tissues in T-cell-dependent or T-cell-independent way. Where T-

cell-dependent activation culminates in the production of antigen-specific and affinity-matured antibodies (26), T-cell-independent pathway activates polyreactive, low-affinity antibodies (30). Acquired immunity has an important role in preserving host-microbe homeostasis, the essential feature of which is the production and secretion of IgA (30).

There is a separation between local and systemic humoral immunity against gut infections (31). The antibodies present in serum may not be reflective of the local antibody response produced at the mucosal level, but antibodies in serum are nevertheless sometimes also used to characterize immune responses to gut infections (32). Antibodies generated in the serum indicate a primed and booster response with a predominance of immunoglobulin G (IgG) that persists for a longer duration than other responses (33, 34). Immunoglobulin A (IgA), that have a half-life of around one week in serum, is produced independently of mucosal IgA during gut infection (31).



1.2.2. IgA in the gut

The plasma cells of the human intestines secrete between 3 and 5 grams of IgA each day. This IgA plays a major role in the protection against pathogens (35).

Gut infections trigger B-cell activation in gut-associated lymphoid tissue (GALT), leading to polyclonal production of T-cell-dependent or independent mucosal antibodies (36). Human B-cells produce two subclasses of IgA in the mucosa, IgA1 and IgA2, whereas IgA1 is predominant in serum. Due to structural differences, IgA2 is more resistant to bacterial proteases than IgA1 in the gut, thus making it well adapted for functioning in a mucosal setting. IgA2 is present in abundance

at the secretory effector sites and predominates the distal gut (37). Here its production is dependent on the bacterial load. Along with locally produced IgA, other serum IgA may also leak onto the mucosal surfaces during an infection, leading to an increased total IgA.

1.2.3. The process of transcytosis

In the gut lamina propria, plasma cells mainly produce dimeric IgA (Figure 1) (35). Dimeric IgA is a combination of two monomeric IgA molecules bound by J peptide chain. During secretion of IgA, locally produced dimeric forms of IgA binds to a polymeric immunoglobulin receptor (pIgR) on the basolateral surface of epithelial cells and it is transferred to the mucosal surface through transcytosis (26). At the apical end of the epithelial cell, the pIgR is cleaved and the part that remains attached to the dimeric IgA is called the secretory component (35). The IgA with the secretory component is known as secretory immunoglobulin A (SIgA).

1.2.4. Secretory immunoglobulin A (SIgA)

Production of SIgA is the hallmark of a mucosal adaptive immune response, it is present in the gut lumen and interferes with the colonization of microbes (26). It is a form of antigen-specific antibody with functional superiority over monomeric IgA or IgG and exists in the gut in a highly stable form (30, 38). Therefore, a rational approach to gauge the gut immune response is to measure SIgA levels (32).

The role of SIgA in the gut is multi-faceted. Coating of microbes by SIgA can result in inhibition of bacterial growth by limiting their utilization of nutrients, restrict bacterial motility, and enchain and random aggregate bacterial cells, thus facilitating their removal from the gut through

peristalsis (26, 39). In addition, it is needed for neutralizing surface-exposed or secreted virulence factors that pathogens use to breach mucosal membranes and leading to epithelial invasion (38).

1.2.5. Other immunoglobulins in the gut

Like SIgA, the pentameric form of IgM, which also incorporates the J chain, binds to pIgR and is exported to the apical surface and released as SIgM. Together, they constitute the first-line humoral defence system of the gut. SIgM play an important role in immune exclusion, inhibit surface colonization, and hinders the penetration of harmful exogenous virulence factor proteins. SIgM also mediates toxin neutralization. In individuals with selective IgA deficiency, SIgM play a major compensatory role in host defence (40).

1.2.6. Immune response to glycosylated antigens

Little is known about what effect glycosylation has on the antibody response to bacterial protein virulence factors. Glycosylation could mask important functional parts of the proteins, it could deceive the immune system to target functionally less important parts of the virulence factor, it could help to reduce cross-reactivity induced by previous infections by masking conserved epitopes (23). Antigenic potential and immune response against glycosylated antigens require further probation.

2. RATIONALE

In 2015, all United Nations member states adopted ‘The Sustainable developmental Goals’ as an attempt to attain a better, healthy, and sustainable future for all. In this agreement, Goal 3 is dedicatedly related to health, with Target 3.2 emphasizing ending preventable deaths of neonates and children under 5 years of age, and Target 3.b supporting the development and research for vaccines and medicines for communicable and non-communicable diseases, especially for those affecting LMIC populations.

Among the most important communicable diseases, diarrhoea continues to be one of the leading causes of child mortality in LMICs (41) causing more than 400 000 deaths and over 1 billion episodes of illness each year. Additionally, diarrheal diseases account for 40 million disability-adjusted life years (DALYs) from new cases, increasing almost 40% to 55 million when also including short- and long-term effects (42). ETEC is one of the most common causes of diarrheal illness of bacterial aetiology (43), where ETEC alone contributes to about 50,000 deaths and 75 million episodes of diarrhoea annually (44).

ETEC diarrhoea in children is usually characterized by an acute onset of watery diarrhoea (45). It may also be accompanied by nausea, vomiting, lethargy, abdominal cramping, dehydration, decreased urination, and fever. Moreover, the child may be unable to feed, and if not rapidly rehydrated, may die from severe dehydration. Inability to access health care, therefore, plays a major role in the prognosis of this seemingly trivial illness.

Recurrent episodes of diarrhoea, including from ETEC infections, may also carry long-term sequelae such as malnutrition, stunting, environmental enteropathy (46), and delayed cognitive development (47).

Since there is a relatively high prevalence of malnutrition among children in LMICs, repeated attacks of diarrhoea can further aggravate this burden. Diarrhoea predisposes children to various infective illnesses owing to malnutrition and improper uptake of micro-and macronutrients (48). This is a common occurrence in children from these regions, especially those belonging to low socioeconomic status. Factors like poor nutrition, poverty, inability to access health care, and lack of education compound these problems.

Another factor that adds to this adversity is non-judicious use of antibiotics during diarrhoea, typically in LMICs, that may not only cause adverse drug reactions but also leads to antibiotic resistance, as enteric diseases are among the leading reasons for antibiotic usage in these areas (49).

Consequently, access to effective ETEC vaccines is imperative to help improve health and lower the disease burden among LMIC children. Significant success in reducing the diarrhoeal burden has been witnessed from the introduction of rotavirus vaccination, which has dramatically altered the paediatric aetiology of diarrhoea by not only protecting against rotavirus but also against other aetiologies of diarrhoea (43). In the light of this advancement, in 2020, the World Health Organization (WHO) issued a consensus statement saying that to “develop a safe, effective, and affordable ETEC vaccine that reduces mortality and morbidity due to moderate to severe diarrhoeal disease in infants and children under 5 years of age in LMICs” is now a primary strategic goal (50). The intended effects of vaccinating against ETEC are not just to reduce morbidity and mortality due to the ETEC diarrhoea, but also to reduce the spread of antibiotic resistance, reduce the financial burden on the healthcare providers, and minimize the long-term complications associated with diarrhoea.

As part of the effort to develop effective vaccines against ETEC, there is a need to improve our understanding of the body's responses to these infections, and to identify potential immune correlates of protection that can be targeted through vaccination. Studying these aspects of human ETEC infection and diarrhoea is complicated by the lack of suitable animal models, so controlled human infection models (CHIMs) are used instead. In ETEC CHIM studies, human volunteers are experimentally infected with wild-type ETEC strains in order to study responses. Such studies have already shown that volunteers who had been experimentally infected with a wild-type ETEC strain were strongly protected against symptomatic infection when rechallenged with the same strain (32, 51). Additionally, a diminished or decreased antibody response was seen against vaccine antigen contents as compared to their wild-type equivalents (52), possibly due to the way they are recognized by the immune system.

In our review paper on immune responses to ETEC infections (1), we emphasized that subunit vaccines based on recombinantly produced ETEC antigens may lack some of the immunologic signatures that are found when the antigens are naturally produced by ETEC. Recombinant antigens may, therefore, potentially give a sub-optimal immune response when used in vaccines. Wild-type ETEC tends to glycosylate important non-classical virulence factors that are associated with membrane vesicles, including YghJ (21). Antibodies produced in response to glycosylated antigens may target these glycosylated residues, and could, therefore offer a stronger or more effective protective immune response than naked YghJ (23).

There is a huge gap in our knowledge about how the humoral immune system responds to glycosylated antigens, and improving our understanding of these responses may also help us to develop broadly effective vaccines against these pathogens (53).

Even though YghJ is a highly conserved *E. coli* virulence factor, data on immune responses to YghJ during infections with pathogenic *E. coli* in humans are scarce. Some data are available from serum analyses of samples collected during ETEC CHIM studies (15, 19, 54) and from natural infections in LMIC children (55). However, intestinal antibody responses have yet to be evaluated.

Therefore, in the present study, we focused on analysing lavage as well as serum samples for YghJ-specific IgA responses in volunteers who have been experimentally infected with a wild-type ETEC strain. By using glycosylated and non-glycosylated YghJ as test antigens, we aimed to determine to what extent the IgA response to YghJ during an experimental infection targets glycosylated and non-glycosylated epitopes on YghJ.

3. MATERIALS, METHODS, AND METHODOLOGICAL CONSIDERATIONS

3.1. Brief description of the experimental ETEC infection study

In the period between 2014 and 2018, 21 volunteers, including 2 males and 19 females, were recruited and experimentally infected with wild-type ETEC strain TW10722 at Haukeland University Hospital. This was part of a project at the University of Bergen to develop a human challenge model that could be used for testing new ST-based ETEC vaccine candidates (56), and details of the study have been described by Sakkestad *et al.* (15). Lavage and serum samples collected from before and 10 days after ingesting the ETEC were stored and used in this study. The volunteers recruited were between 18 and 40 years of age, healthy, immunocompetent, had normal serum immunoglobulin levels, had normal findings on physical examination, and enteropathogens were absent in their stools.

They were briefed about the implementation of this project, the risks of volunteering, the potential impact of isolation, and the procedures that were to be performed during its implementation.

3.2. Experimental infection of the volunteers

The volunteers fasted overnight, and, in the morning, they drank sodium bicarbonate to neutralize stomach acids shortly before ingesting bicarbonate buffer containing ETEC strain TW10722. The volunteers were observed for the development of diarrhoea and any other signs or symptoms. The time and date of all stool evacuations, as well as the weight and looseness of each stool, were recorded. The results were used to assess the presence of diarrhoea, its severity, incubation period, and a maximum weight of stools and their volume during any 24-hour period. Diarrhea was defined

as a volunteer producing 1 loose or liquid stool of ≥ 300 g, or ≥ 2 loose or liquid stools totalling ≥ 200 g during any 48-h period within 5 days post-infection. To clear the infection, volunteers were treated with ciprofloxacin within 24 hours of becoming severely ill, or within 120 hours after dose ingestion, whichever came first. Three consecutive stool samples were verified to be ETEC negative prior to discharge from the hospital. Total hospital stay ranged between 5 to 9 days.

3.3. Infecting strain

ETEC strain TW10722 (O115:H5; GenBank BioProject: PRJNA59745) was isolated in 1997 in Guinea-Bissau from a 15-month child suffering from acute diarrhoea. The strain expresses the two colonization factors CS5 and CS6 along with STh. It does not express heat-labile toxin. It is a good representative of an ETEC family that is often associated with moderate and severe childhood diarrhoea in LMICs.

3.4. Sampling methods

Venous blood samples were obtained after an overnight fast prior to infection at day 0 (the day the volunteer ingested the dose) and day 10. Serum samples were prepared after sample coagulation in a tube for 90 minutes at room temperature followed by centrifugation at $2000 \times g$ for 10 minutes before storage at -70°C .

Intestinal lavage sampling was performed on the day of the screening (usually 2 weeks before dose ingestion) and on day 10. To perform the lavage, the subjects drank large volumes of Laxabon. Laxabon is an osmotic solution that is routinely used to clean the colon prior to colonoscopy, and it stimulates the passage of watery stools. It is a salt solution like oral rehydration salt, except these salts are not readily absorbable by the intestine, which otherwise would increase urine output but not cause diarrhoea. and. At least 100 mL of lavage specimen was collected for future analyses

and a protease inhibitor was added to prevent proteolytic degradation of antibodies in the samples, before immediate freezing at -70°C .

The content of total IgA antibodies in lavage fluid can be quite variable. Moreover, SIgA in the sample is liable to undergo proteolytic degradation during the process of collecting and storage. Even then, measuring antibody-mediated protection from infection in the small intestinal fluid is considered the “gold standard” (32) as mucosal immunity is the most reliable indicator of the protective immune response against gut infections.

3.5. Materials

A list of equipment, reagents, and buffers used in this thesis is as following.

3.5.1. Equipment

Table 1. List of equipment with catalogue number and manufacturer information

Item	Catalogue number	Manufacturer, Provider
Micro-tube 2 mL PP	72.694.006	Sarstedt, Germany
Propylene tubes, 15 mL, 120x17 mm	62.554.502	Sarstedt, Germany
Disposable cuvettes	634-0676	VWR, Germany
Whatman® Syringe Filter, 25mm, Puradisc, 1 µm	6783-2510	Whatman, UK
Whatman® Spartan® HPLC certified syringe filters 0.45 µm	WHA10463110	Merck KGaA, Germany
Millex-GS Syringe Filter Unit, 0.22 µm	SLGS033SS	Merck KGaA, Germany
Eppendorf® Bio-photometer	6131	Eppendorf, Germany
Nunc™ 96-Well Polystyrene Round Bottom Microwell Plate	262162	Thermo Fisher Scientific, U.S.A
Thermo shaker (Plate shaker)	PST-60HL-4	BioSan, Germany
Pipette tips (10 µl, 200 µl, 1000 µl)		Sarstedt, Germany
Eppendorf® Centrifuge 5800 (5810R)	Z605263	Eppendorf AG, Germany
Eppendorf® Centrifuge 5415D	EP-5415D	Eppendorf AG, Germany
Flow cytometer BD LSR Fortessa™		BD Biosciences U.S.A
Filter plates Multiscreen HTS HV 0.45 µm 96-well	MSHVS4510	Merck KGaA, Germany
BD CBA Human IgA Flex Sets	558681	BD Biosciences, USA
Micro BCA™ Protein Assay Kit	23235	Thermo Fisher Scientific, U.S.A

3.5.2. Reagents

Table 2. List of reagents with catalogue number and manufacturer information

Item	Catalogue number	Manufacturer, Provider
Carboxylated Beads Cyto-Plex™ 4µm	FM4CR02, FM4CR07	Thermo Fisher Scientific, U.S.A
Poly (ethylene glycol) 2-aminoethyl ether acetic acid (PEG polymer)	757888	Sigma-Aldrich, Germany
N-(3-dimethylaminopropyl)-N'-ethyl carbodiimide HCl (EDC)	161462	Sigma-Aldrich, Germany
N-hydroxysulfosuccinimide (Sulfo-NHS)	24510	Thermo Fisher Scientific, U.S.A
Tris Hydrochloride (Tris-HCl)	10812846001	Sigma-Aldrich, Germany
Alexa Fluor® 488 Affinipure Goat Anti- human serum IgA antibody	109-545-011	Jackson Immuno Research, UK
Glycosylated YghJ-protein (TW10722)	Provided by partner	GlyProVac, Denmark
Non-glycosylated YghJ-protein (TW10722)	Provided by partner	GlyProVac, Denmark
2-Morpholinoethanesulfonic acid monohydrate (MES) powder	145224-94-8	Merck KGaA, Germany
Bovine serum albumin (BSA)	A3311	Sigma-Aldrich, Germany
Tween® 20	P1379	Sigma-Aldrich, Germany

3.5.3. Buffers

Table 3. List of buffers used in the thesis

Names	Contents and pH
Dulbecco's Phosphate Buffer Saline (PBS)	8 g NaCl, 0.2 g KCl, 1.44 g Na ₂ HPO ₄ , 0.24 g KH ₂ PO ₄ in end volume 1 L ddH ₂ O ; pH 7.4 at room temperature
PBS with 0.3 M NaCl (10 mL)	20 µL of 1M NaH ₂ PO ₄ , 180 µL Na ₂ HPO ₄ , 600 µL 5 M NaCl, 9.2 mL ddH ₂ O
Assay buffer (10 mL) (PBS with 1 % BSA, 0.05 % Tween-20)	8950 µL PBS, 1000 µL 10 % BSA (in PBS), 50 µL 10 % Tween-20 (in PBS) ; pH 7.4 at room temperature
2X assay buffer (10 mL) (contents are double in concentration than assay buffer)	162 µL 1 M Na ₂ HPO ₄ , 29.4 µL 1 M KH ₂ PO ₄ , 548 µL 1 M NaCl, 54 µL 1 M KCl, 2000 µL 10 % BSA (in ddH ₂ O), 100 µL 10 % Tween-20 (in ddH ₂ O) in 7.1 mL ddH ₂ O ; pH 7.4 at room temperature
1M MES Buffer (2-(N-morpholino)ethanesulfonic acid sodium salt)	3.904 grams MES powder, 0.4 mL 5M NaOH (check while mixing so pH does not exceed the prescribed limit), total volume to 20 mL by adding ddH ₂ O ; pH 5.5
50 mM MES	1 mL 1 M MES buffer, pH 5.5, 19 mL ddH ₂ O
Cyto-plex storage buffer (1.2 mL)	2.4 µL 1M NaH ₂ PO ₄ , 21.6 µL 1M Na ₂ HPO ₄ , 120 µL 10 % BSA, 6 µL 10 % Tween-20, 72 µL 5 M NaCl, 972 µL ddH ₂ O

3.5.4. Flow cytometer

Flow cytometry is widely used for analysing individual cells and other particles. A flow cytometer works by the principle that when fluorescent dye-labelled cellular components or particles pass in front of a laser, they absorb light and are excited, emitting visible fluorescence. The resulting fluorescence is then recorded when cells or particles pass one by one by several detectors placed along the length of the sample stream.

For forward scatter (FSC) measurements, the detector is in line with the light beam, whereas for side scatter (SSC) measurements, the detector is placed perpendicular to the beam of light. All three dimensions area, width, and height can be measured. This combination allows the determination of the size or volume of the particles/cells and their granularity (57).

3.5.4.1. Flow Cytometer settings and fluorochromes

Laser (wl)	FSC	SSC	Blue (488)	Red (700)
Filter LP	-		505	710
Filter BP	488/10		530/30	730/45
Fluorochrome used	-		Alexa flour® 488	Firefli Red
Voltage	300	240	380	410
Target measurement	Beads		IgA antibodies	Cyto-Plex beads
Size threshold	11,000			

Table 4. Settings used in the Fortessa Flow cytometer.

The YghJ proteins were coupled to Cyto-Plex beads that had different levels of Firefli red fluorochrome. The red laser excited this fluorochrome and different bead populations and, consequently, protein types, could be easily gated based on the bead emission strength at 730 nm.

To quantitate IgA bound to YghJ-coupled beads, we used Alexa Fluor® 488 Affinipure Goat Anti-human serum IgA antibody as a secondary antibody, which could be detected by emission around 518 nm. The details of fluorochromes used and flow cytometer setting are given in Table 4.

3.5.5. Computer software used

For data acquisition, Florescent-activated cell sorting (FACS) Diva acquisition software version v9.0 (BD Biosciences, U.S.A) was used.

Flow cytometry data were processed in FlowJo v10.4.2 (BD Biosciences, U.S.A) software. FlowJo is a tool for viewing and analysing flow cytometry data. It allows the generation of graphs and statistical reports to uniformly analyse the whole experiment. It can also assist with data management, analysis, and report generation.

Microsoft Word and Microsoft Excel (both Microsoft Corp, U.S.A) were used to document the data generated from the experiments. GeoGebra classic (Linz, Austria) was used to make plot standard curves. GraphPad Prism 9 (GraphPad Software Inc, U.S.A) was used to plot all other graphs and for performing the necessary statistical analyses. Gravit Designer (Corel Corp, Canada), Microsoft Paint, and Microsoft PowerPoint (both Microsoft Corp, U.S.A) were used to make illustrations.

3.6. Methods

3.6.1. Preparation of lavage samples

Before analyses, the stored samples were taken out of the freezer and thawed in the fridge to be filtered. Samples were first centrifuged at 16,000 x g (Eppendorf[®] Centrifuge 5415D) for 3 minutes and the supernatant was collected in a 10 mL syringe. It was serially filtered through 1 µm (Whatman[®] Syringe Filter, 25 mm, Puradisc), 0.45 µm (Whatman[®] Spartan[®] HPLC certified syringe filters), and finally 0.2 µm (Millex-GS Syringe Filter Unit) filters. The samples were then aliquoted and stored at -70 °C until needed.

3.6.2. Antigen production

Recombinant non-glycosylated and glycosylated YghJ based on the TW10722 genetic sequence for YghJ were kindly provided by our collaborative partners in this project, Anders Boysen and Ann Zahle at GlyProVac ApS. The cloning, production, and purification of these proteins are detailed in the manuscript. Both the native, glycosylated YghJ and the non-glycosylated YghJ were bound to 3xFLAG tags that had been used to immobilize the protein during purification through the use of anti-FLAG antibodies.

3.6.3. Quantitation of proteins

YghJ protein concentrations were determined by using the Micro BCA protein assay kit, which has a linear concentration range of 0.5 µg/mL to 40 µg/mL. A standard row was made by diluting Bovine Serum Albumin in PBS in nine 1.5 mL Eppendorf tubes, as indicated in Table 5.

Vial	Volume of concentrated BSA	Volume of PBS	Final BSA Concentration
A	20 μ L (from standard)	180 μ L	200 μ g/mL
B	80 μ L from A	320 μ L	40 μ g/mL
C	200 μ L from B	200 μ L	20 μ g/mL
D	200 μ L from C	200 μ L	10 μ g/mL
E	200 μ L from D	200 μ L	5 μ g/mL
F	200 μ L from E	200 μ L	2.5 μ g/mL
G	200 μ L from F	300 μ L	1 μ g/mL
H	200 μ L from G	200 μ L	0.5 μ g/mL
I	Add buffer only	200 μ L	0 μ g/mL

Table 5. Shows dilution row of proteins for standard curve.

The assay was prepared in Nunc™ 96-Well Polystyrene Round Bottom Microwell Plate. Each well contained 50 μ L of BCA reagents and 50 μ L of protein solution to be measured. The plate was covered and incubated at 60°C in an incubator for 1 hour followed by absorbance measurements with a 562 nm filter. All the samples were measured within 10 minutes.

3.6.4. Covalently coupling YghJ to beads

Antibody analyses of lavage and serum samples were done by using a flow cytometry bead assay. The method was chosen since it allowed for multiplexing assays to measure several analytes in a single assay, and the assays usually give a comparatively low background, a broad dynamic range

of measurements, and are inexpensive and quick to perform once the beads have been conjugated (58). Our assay is based on fluorescently labelled carboxylate microspheres (Cyto-Plex beads) that serves to anchor the antigen of interest, which in our case were glycosylated and non-glycosylated versions of YghJ. By incubating YghJ-coupled beads with antibodies in samples collected from the volunteers and subsequently quantifying the bound antibodies, we obtained a measure of the anti-YghJ levels in the samples.

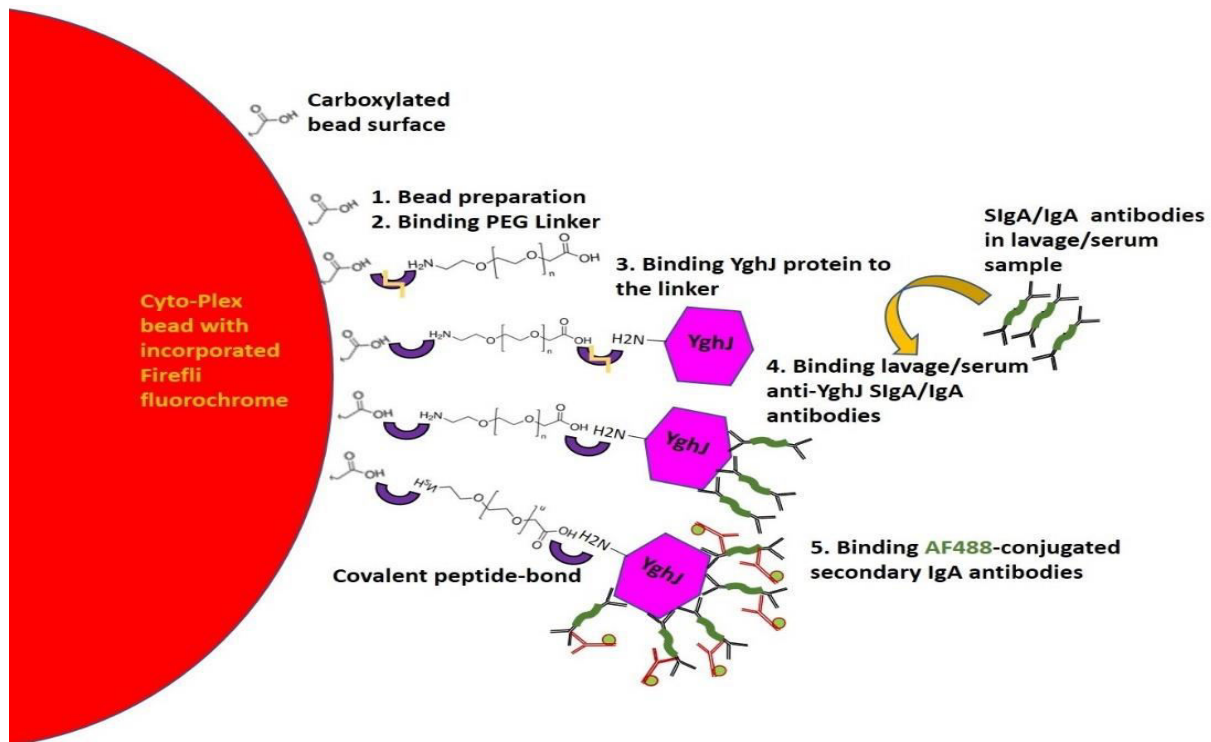


Figure 2. Diagrammatic presentation of steps involved in the preparing of beads and performing the multiplex beads immunoassay. It shows sequential activation of Cyto-Plex beads and covalent linking of PEG linker followed by binding of YghJ antigen. Antibodies from lavage/serum sample then bind to the antigen, which in turn bind to fluorescent secondary IgG antibody.

We received the YghJ proteins in a PBS buffer containing Triton-X100, which is added to keep YghJ from precipitating. Since this detergent is attracted to polystyrene beads and, therefore, prevents YghJ from coming into close proximity of the beads, our initial attempts to couple the YghJ antigen directly to the Cyto-Plex beads failed. We also coupled anti-FLAG antibodies to the

beads before incubating with YghJ, but the YghJ would not stay immobilized. We finally had success by first coupling long (~16 nm) Poly-ethylene glycol (PEG) linkers to the beads, and then coupling YghJ to the end of these linkers. The rationale behind using this linker was that it would extend the attachment points far beyond the surface of the beads and beyond the layer of Triton-X100 that would inevitably coat the beads. One end of the linker has a primary amino residue, similar to the protein N-terminal, while the other end has a carboxyl residue, similar to those on the surface of the beads (Figure 2). For this coupling, we used EDC (1-ethyl-3-[3-dimethylaminopropyl]carbodiimide) and Sulfo-NHS (sodium N-hydroxysulfosuccinimide) to create amine-reactive esters of the carboxyl residues. The linkers were first coupled to the activated beads, and YghJ was subsequently coupled to the activated linkers.

All the buffers needed were prepared according to the table, above. In this procedure, we first quantitated glycosylated YghJ (gYghJ) and non-glycosylated YghJ (nYghJ) as described above, before coupling to two different bead populations (L2 and L7) as follows. Bead concentrations were determined by using a Bürker chamber.

The filter membrane at the bottom of the wells of a Multiscreen HTS HV 0.45 μm 96-well filter plate were wetted by adding 100 μL 50 mM MES buffer, and the plate was subsequently centrifuged at $300 \times g$ for 45 sec to remove excess liquid. We then mixed 150 μL 50 mM MES buffer and 50 μL (approximately 8 million) Cyto-Plex beads in each well and removed the liquid by centrifugation at $50 \times g$ for 45 seconds. Then, the beads were then washed with 200 μL 50 mM MES buffer, mixed by pipetting and by scraping the bottom with the pipet tip to dislodge any stuck beads, and centrifuged at $50 \times g$ for 45 sec at room temperature. This last wash step was performed twice at the end of each of the following reactions.

To activate the beads, we added 160 μL 50 mM MES buffer, 20 μl freshly prepared 50 $\mu\text{g}/\mu\text{l}$ EDC, and 20 μl freshly prepared 50 $\mu\text{g}/\mu\text{l}$ Sulfo-NHS to each well, mixed, and incubated at room temperature for 20 mins, shaken at room temperature on a Thermo-shaker (PST-60HL-4) (3 mm \emptyset) at 600 rpm. Following centrifugation at 50 x g for 45 seconds and two washes, we added 200 μL 50 mM MES buffer containing 2 mg of the PEG linker and mixed by carefully pipetting and filter scraping. Pipetting after this step was done slowly as the long linkers attached to beads might break due to the hydro-shearing effect of vigorous pipetting. After incubating the plate on the shaker at room temperature for 2 hours, the plate was centrifuged again at 50 x g for 45 seconds and washed thrice, as before. To couple YghJ to the end of the bead-coupled linkers, we repeated the activation step from above, including adding 160 μL 50 mM MES,

20 μl each of freshly prepared 50 $\mu\text{g}/\mu\text{l}$ EDC and Sulfo-NHS. After the 20 min incubation, centrifugation and washing, we added 200 μL 50 mM MES containing 18 μg YghJ, while carefully scraping the bottom and walls of the wells to ensure resuspension of beads in the mixture. The plate was incubated at room temperature for 2 hours initially (600 rpm, 3 mm \emptyset), then moved to a dark, cold room (4°C) for overnight incubation. The next morning, wells were washed with 200 μL PBS twice and the beads were resuspended and transferred to Eppendorf tubes in 400 μL Cyto-Plex storage buffer (see contents table), followed by determination of bead concentration by using a counting chamber, and storage at 4°C. Lastly, 1.5 μL 1 M Tris-HCl, pH 8, was added to the bead mixture after ca. 24 hours to neutralize any remaining unreacted sites on the beads and linkers.

3.6.5. Flow cytometric bead immunoassay

To estimate the YghJ-specific IgA antibody levels in the lavage and serum samples, a multi-plex bead-based flow cytometric assay was performed. The lavage and serum samples were thawed on ice before the experiments.

Wells in a Multiscreen filter plate was wetted by adding 100 μL assay buffer before centrifugation at $300 \times g$ for 45 sec. A mixture of 5000 beads of each nYghJ- and gYghJ-conjugated beads for each assay was prepared in 50 μL assay buffer and added to the wetted wells. Prior to this, lavage samples had been diluted 1:1 in 2X assay buffer to adjust the sample's pH and salt content, while the serum samples were diluted 1:50 in assay buffer. We added 50 μL of the diluted samples to the 50 μL bead solution in the wells (1:4 and 1:100 final dilution of lavage and serum, respectively), before incubating the plate at room temperature for 30 minutes at 600 rpm on our microplate shaker. The plate was then centrifuged at $50 \times g$ for 45 seconds and washed twice with 200 μL assay buffer as described for the protein coupling procedure in the previous section.

We then added 50 μL Alexa Fluor® 488 Affinipure Goat Anti-human serum IgA antibody diluted 1:200 for lavage (1:400 for serum) in assay buffer to each of the wells. It was mixed thoroughly with the beads by careful pipetting. The plate was incubated again on the microplate shaker at 600 rpm for 30 minutes at room temperature, followed by centrifugation at 50 g for 45 seconds and two washes. Finally, the beads were resuspended in 200 μL assay buffer and analysed on the flow cytometer which was equipped with a microplate reader for fast processing.

3.6.6. Total IgA quantitation

Since the concentration of antibodies in the lavage samples will inevitably vary depending largely on how much laxative the volunteers drink, we determined the IgA concentrations in all our lavage samples by using the BD Cytometric bead array (CBA) Human IgA Flex Set kit (BD Biosciences, San Jose, CA).

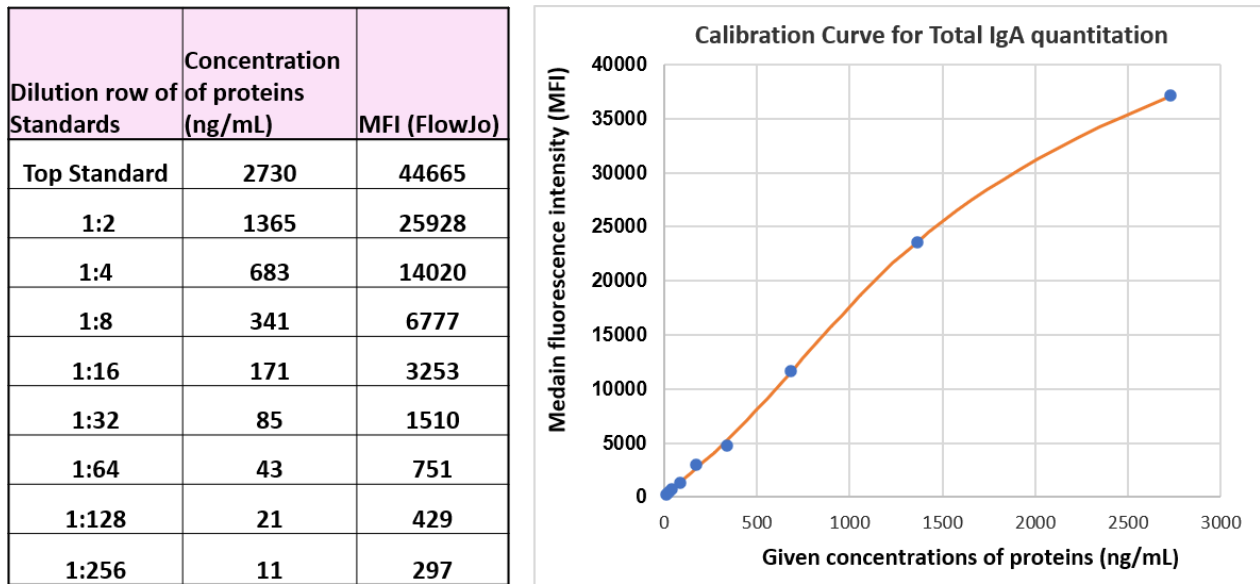


Figure 3. Show concentration of given proteins at specific dilutions projected against MFIs obtained from the FlowJo to obtain a standard curve for measurement of total IgA in the samples from MFI values.

In these assays, lavage samples were thawed on ice, while the lyophilized IgA standard was diluted in a series ranging from 2730 ng/mL to 10.7 ng/mL (1:256) in PBS, and with PBS as the negative control, as shown in Figure 3.

In this assay, we wetted the wells of a Multiscreen HTS HV 0.45 μm 96-well filter plate with 200 μL PBS, followed by centrifugation at $300 \times g$ for 45 sec and the addition of 50 μL PBS. Lavage

samples from day 0 and day 10 from the volunteers were diluted 1:1000 in PBS, and 50 μ L were added to each well containing 50 μ L PBS, giving a final concentration of 1:2000. We then added 50 μ L of diluted Capture beads (1.0 μ L beads in 49 μ L PBS) to each well and incubated for 1 hour at room temperature. After centrifugation at $50 \times g$ for 45 sec and washing the beads twice, each done by adding 200 μ L assay buffer followed by centrifugation at $50 \times g$ for 45 sec, we added 50 μ L of diluted PE detection reagent (1.0 μ L reagent in 49 μ L PBS) and incubated for 2 hours at room temperature. After washing twice, the beads were resuspended in 200 μ L assay buffer, and 150 μ L were transferred to a new microplate and analyzed on a flow cytometer.

Median Fluorescence intensity (MFI) estimates of the standards and lavage samples were obtained by gating in FlowJo with settings explained later (section 3.6.8.2). A standard curve was plotted in which the MFI estimates derived from the standards were plotted against the known IgA concentrations (Figure 3). This standard curve was then used to calculate the IgA concentration in the lavage samples.

3.6.7. Specificity Assay

To estimate the proportion of the YghJ-specific IgA antibodies that target glycosylated epitopes, we performed specificity assays on serum and lavage samples that had been collected on day 10. In these assays, the samples were pre-incubated with either 1) glycosylated YghJ, to neutralize all anti-YghJ antibodies from the samples, 2) non-glycosylated YghJ, to neutralize all anti-YghJ antibodies that do not target glycosylated epitopes on YghJ, and 3) assay buffer, which does not neutralize any anti-YghJ antibodies, before being analysed in the flow cytometric bead immunoassay described previously.

The samples were thawed on ice before being diluted 1:2 (for lavage) and 1:100 (for serum; for fold change estimation, we had used 1:50) in assay buffer, and triplicates of 50 μ L were transferred to individual wells on a microplate. To the wells of each triplicate, we added 1 μ g glycosylated YghJ, 1 μ g non-glycosylated YghJ, and assay buffer, respectively. After incubation on a microplate shaker (3 mm \emptyset) at 600 rpm for 30 minutes at room temperature, the triplicate samples were analysed as described above.

3.6.8. Gating strategy

3.6.8.1. Gating strategy for YghJ-specific IgA in lavage and serum samples

Gating is the sequential selection of data from flow cytometry analyses. Here, we use gating to isolate data from specific bead populations in our multiplex assay, which enables us to estimate the anti-YghJ levels in our samples.

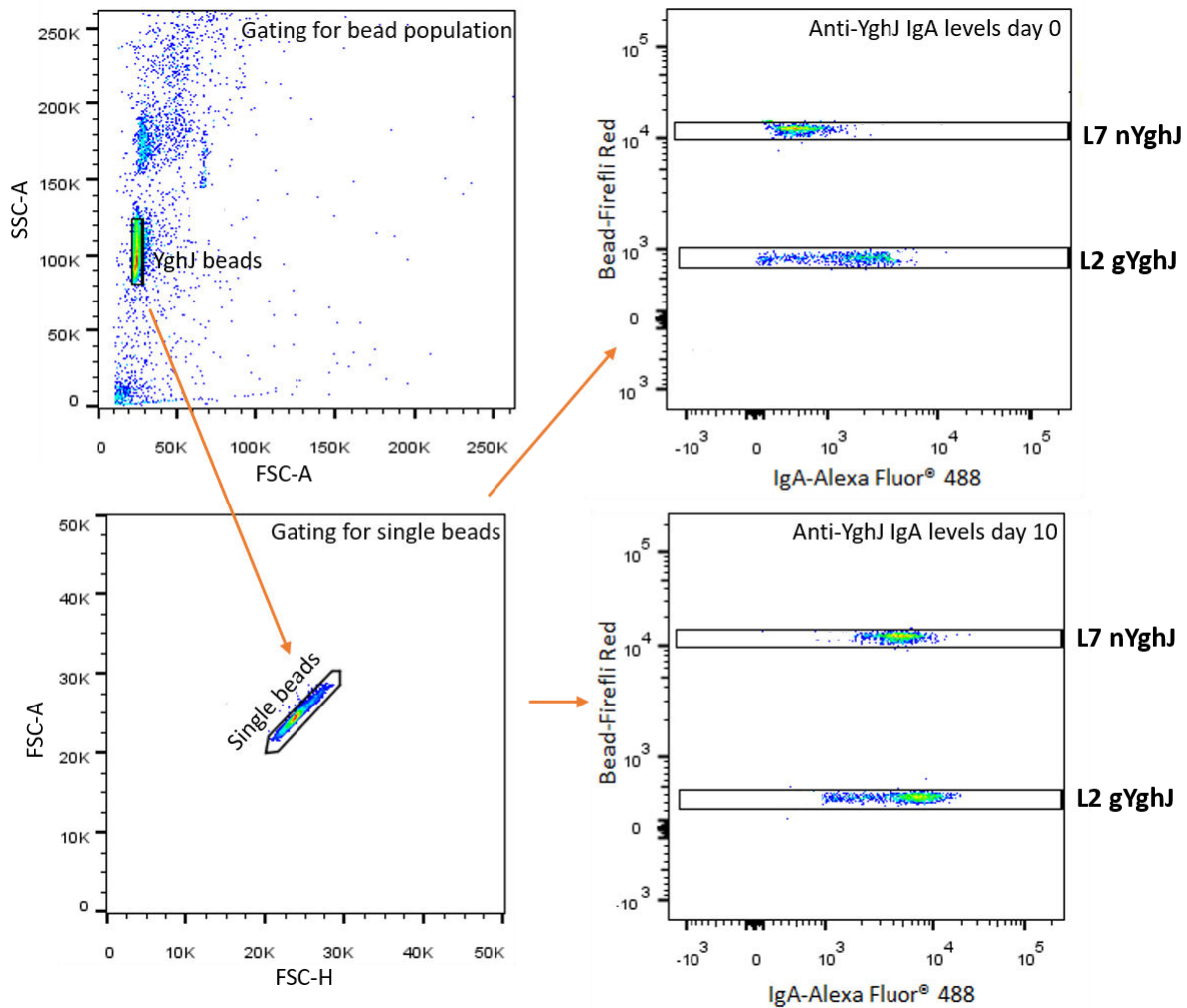


Figure 4. Representative gating strategy. Gating employed in FlowJo to calculate median IgA values for day 0 and day 10 samples in a serum specimen.

In this gating, we first isolated data from single beads, thus ignoring doublets and debris in the assay, by gating in forward scatter area (FSC-A) and side scatter area (SSC-A), followed by gating on forward scatter height (FSC-H) and FSC-A (Figure 4) Finally, data from beads coupled with the different variants of YghJ can be separated by gating on the Firefli red fluorescence levels and on the Alexa Fluor® 488 fluorescence. Due to the differences in intensities of Firefli fluorescence, L2 was shown at the lowest point on the y-axis and L7 at the highest. The gate was placed extending the entire length of the x-axis. The median fluorescence intensity (MFI) of Alexa Fluor® 488 of each bead population was then used as an estimate of the anti-YghJ IgA level.

3.6.8.2. Gating strategy for Total IgA in lavage samples in FlowJo

For the IgA quantitation assay, we gated the bead data on FSC-A and SSC-A to separate out bead population from debris in the assay. Then “Single beads” were selected by gating on FSC-A and FSC-H. Lastly, the bead fluorescence and the PE channels were used to gate bead data.

3.6.9. Data generation and analyses

3.6.9.1. Standard curve for lavage and serum samples

Since the MFI values are not likely to be directly correlated with the actual IgA levels in these samples, we generated a reference standard that can be used to normalize our data from the flow cytometry assays.

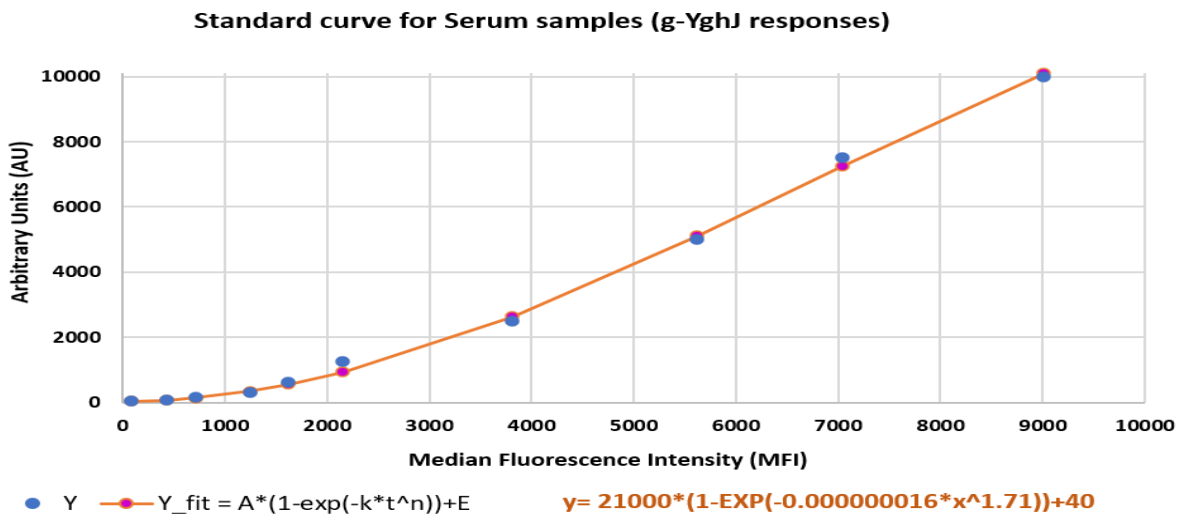


Figure 5. Representative standard curve. Shows standard curve for anti-gYghJ obtained by serial dilution of a strongly positive serum sample.

We ran the assay on a dilution series of the two lavage and serum specimens that had the strongest anti-YghJ responses and created curves that could be used to convert all our MFI values to arbitrary units (AUs) (Figure 5) (58). Using these AUs allows better evaluation of the antibody concentrations, and thereby calculation of real differences, in antibody levels.

Separate standard curves were generated for nYghJ- and gYghJ-coupled beads, for both lavage and serum. For lavage serial dilution, the day 10 sample with the strongest MFI was diluted 1:2

(50 μ L lavage in 50 μ L 2X assay buffer) in a vial, mixed well, and then diluted successively 10 times 1:1 with 50 μ L assay buffer, down to a 1:1024 dilution.

The standard curve for serum samples was obtained in a similar manner, except the initial dilution was 1:50, giving 10 dilutions ranging from 1:50 to 1:12800. All dilution series were done in duplicates and both were used in parallel during analyses. The curves were fitted in Excel and GeoGebra.

3.6.9.2. Normalization of IgA levels in lavage specimens

As mentioned above, the concentration of IgA in a lavage sample differs from person to person and from time to time. To allow for comparison of assay results between samples collected on different days, we normalized the estimated YghJ-specific IgA levels in these samples by dividing the IgA levels (in AUs) by the IgA concentration and using this normalized AU (nAU) in our analyses.

3.6.9.3. Lavage and serum samples fold change calculations

We calculated the fold change in anti-YghJ IgA antibody levels between day 0 (i.e., baseline) and day 10 as a measure of the IgA antibody response to YghJ as a result of the infection. Of the 21 volunteers, lavage samples from two volunteers had IgA amounts below the limit of detection at day 0 and day 10 and hence were excluded in the analyses.

For lavage samples, the estimated IgA antibody levels, given as MFI, were first converted to AUs, before conversion to nAUs, as described in the previous section. We used these normalized values when estimating fold-change in YghJ-specific IgA levels.

Serum fold changes were calculated in the same manner for all 21 volunteers, except that we did not normalize the IgA levels first since serum does not have the large variation in antibody levels that is seen in lavage.

3.6.9.4. Lavage and serum specificity assay calculations

To determine the proportion of anti-YghJ IgA antibodies specifically targeting glycosylated epitopes, specificity assays were performed.

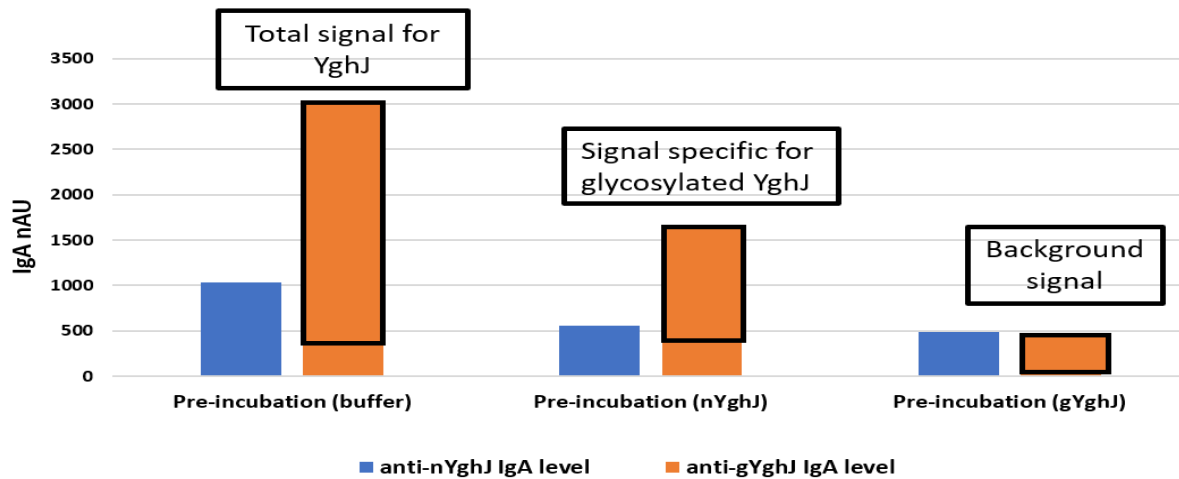


Figure 6. Interpretation of values obtained in the specificity assay.

In this assay, we consider that the native, glycosylated YghJ (gYghJ) presents glycosylated epitopes as well as all other epitopes found in the recombinant, non-glycosylated YghJ (nYghJ). Conversely, the non-glycosylated YghJ does not contain any glycosylated epitopes.

To estimate the proportion of anti-YghJ IgA antibodies that targeted glycosylated epitopes, we set up three bead assays where we pre-incubated the samples with glycosylated YghJ, with non-glycosylated YghJ, and with buffer only (Figure 6). The first of these pre-incubations would

neutralize all anti-YghJ antibodies in the sample, the second would neutralize all anti-YghJ antibodies except those that targeted glycosylated epitopes, while the third would not neutralize any anti-YghJ antibodies. When these three samples are analysed in our bead assay, the first assay would give us the unspecific, background IgA levels. The second assay would give us the levels of anti-YghJ IgA antibodies that specifically target glycosylated epitopes, while the third assay would give us the overall anti-YghJ IgA antibody levels. The proportion of the anti-YghJ IgA that target glycosylated epitopes is then calculated by dividing the estimates from the second assay from those of the third assay, after subtracting the background levels found in the first assay (Figure 6).

3.6.9.5. Statistical Analysis

To estimate the differences in antibody levels between day 0 (baseline) and day 10 for lavage and serum samples, the Wilcoxon signed-rank test in GraphPad prism 9 was used. Testing for differences in fold change between anti-YghJ targeting nYghJ and gYghJ were evaluated in the same way.

Mann-Whitney U test was performed to test differences in IgA levels between volunteers who developed diarrhoea and those who did not. To determine the correlation between lavage and serum IgA antibody levels, Pearson's correlation coefficients were calculated. A p-value of ≤ 0.05 was considered to represent a significant correlation.

4. DISCUSSION

The main discussion points are to be found in the manuscript. Here we elaborate on additional methodological issues, strengths, limitations, and future aspects not mentioned in the manuscript discussion.

4.1. Methodological Aspects

The process of optimizing the assay has been an evolutionary one with due effort and time dedicated to meet the challenges that came with the refinement of the procedure.

4.1.1. Coupling of beads

The proteins we received were too diluted to be used directly for coupling to the beads. We used Vivaspin 500 (Sigma-Aldrich, Germany) centrifugal concentrator to increase the concentration of proteins by adding 50 μ L protein each time and centrifuging in pulses to get rid of the excessive buffer. The concentrated proteins were quantified by using the micro-BCA protein assay kit.

The buffer contained Triton X-100, which is a surfactant that helps to keep YghJ in solution. But most likely owing to its affinity to the polystyrene beads, it prevented the coupling of YghJ directly to the beads. We made several attempts to circumvent this problem.

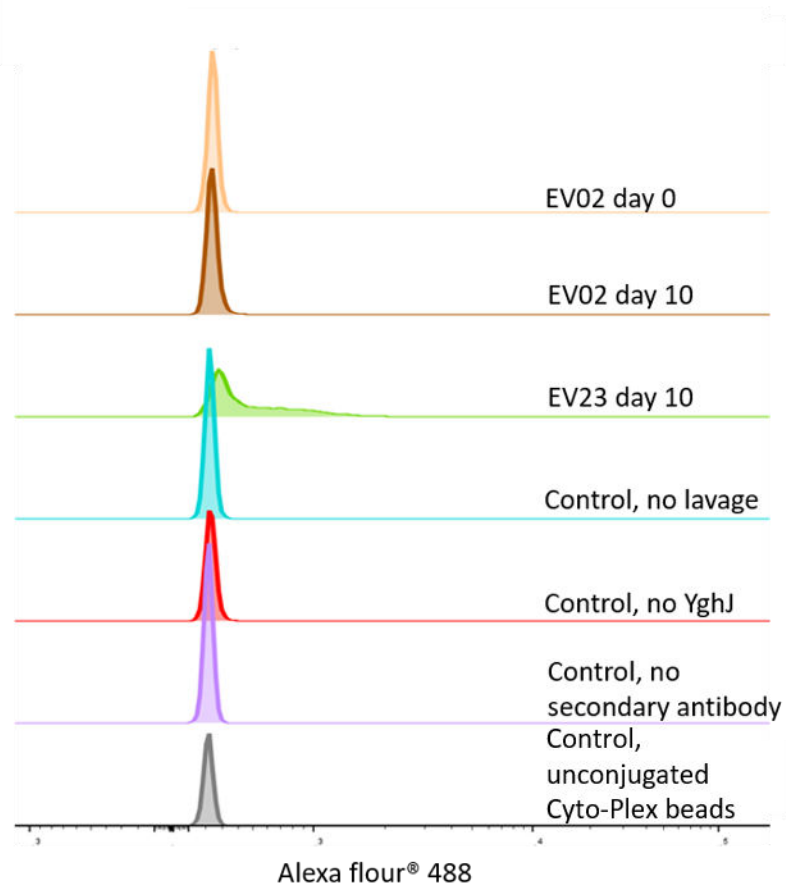


Figure 7. Pilot results of bead assays based on anti-FLAG antibody coupled YghJ. Lavage samples for two volunteers at day 10 and one at day 0 sample were examined. Histograms were derived from FlowJo.

An attempt to couple anti-FLAG antibodies to the beads, assuming the FLAG-tagged YghJ would then bind to these immobilized antibodies even in the presence of Triton, failed. The bead assay signals we got when tested against samples from strong responders were no different from those against our controls, as shown in Figure 7. We do not know whether the antibodies failed to couple to the beads, or whether the binding of YghJ to the antibodies was too weak or unstable.

However, we succeeded in our second attempt, in which we covalently coupled YghJ to the beads via a linker. To characterize these beads, we did a comparison with recombinant YghJ that did not

contain Triton X-100 and could, therefore, be coupled directly to the beads. The results were comparable when tested in flow assays against a small battery of serum and lavage samples.

4.1.2. Testing effects of multiplexing beads

Running our bead assay as a multiplex, where different bead populations presenting different variants of the same antigen posed the question of whether the different bead populations competed with each other for the same anti-YghJ antibodies. In these assays, we also included up to 6 other beads that presented glycosylated and non-glycosylated YghJ that had been isolated from other *E. coli* strains.

Beads in assay	Hexaplex*		Duplex		Monoplex	
	day 0	day 10	day 0	day 10	day 0	day 10
Volunteer EV09						
anti-gYghJ levels	388	27508	266	28342	299	28478
anti-nYghJ levels	329	30160	258	27607	269	25097

Table 6. Testing the effects of multiplexing the anti-YghJ flow cytometric assay. Results are presented as MFI values. * The hexaplex test was run a week earlier than the others.

In these tests, we tested a hexaplex, a duplex, and a monoplex assay to test whether the presence of additional YghJ variants would affect the estimated antibody levels against nYghJ and gYghJ from TW10722. We found that the signal intensities and background signals seemed to increase only slightly when adding more bead variants to the assay (Table 6), suggesting that competition may not be a problem in these assays.

4.1.3. Testing varying assay salinity

Since salinity of the assay buffer will affect the binding strength of the antibodies to YghJ, with lower salinity often tending to increase unspecific binding, we tested the effect of varying the NaCl concentrations in our PBS-based assay buffers.

	day 0			day 10		
NaCl concentration	150 mM	300 mM	600 mM	150 mM	300 mM	600 mM
EV09 (anti-gYghJ)	165	213	244	22453	19408	19035
EV23 (anti-gYghJ)	618	1206	1258	34764	35279	39010
EV09 (anti-nYghJ)	209	297	330	25054	23516	23804
EV23 (anti-nYghJ)	334	992	1310	8387	9760	7741

Table 7. Testing the effects of salinity on the anti-YghJ flow cytometric assay. Results are presented as MFI values.

In these tests, we found that the signals seemed largely unaffected, except that increasing the salt concentration seemed to actually lead to stronger background (presumably) signals, especially in the day 0 samples (Table 7). For this reason, we decided to use 150 mM salt concentration in all our assays.

4.1.4. Optimal dilution of samples

An optimal dilution of both lavage and serum was required to reflect the best estimation of antibody levels in the assays and to minimize the background without overdiluting the samples.

Volunteer EV05	day 0			day 10		
Lavage dilution	1:2	1:4	1:8	1:2	1:4	1:8
anti-gYghJ level	487	276	200	15100	12727	6545
anti-nYghJ level	3240	646	477	22608	18764	9136

Table 8. Data for lavage dilution tests. Antibody levels are shown as MFI.

To identify the optimal dilutions, we made dilution series of different day 10 lavage samples and tested them in the bead flow cytometric immunoassays (Table 8). We aimed to identify the highest dilution that did not result in a large loss of signal strength in weakly positive samples. For the lavage samples, we decided to use a 1:4 dilution for our analyses.

EV30	day 0			day 10		
Serum dilution	1:25	1:50	1:100	1:25	1:50	1:100
anti-gYghJ levels	2466	1722	1042	19347	15312	9795
anti-nYghJ levels	2236	1397	960	20764	14652	8543

Table 9. Data for serum dilution tests. Antibody levels are shown as MFI.

Similarly, for serum samples, several dilutions were tried before we settled for a 1:100 dilution, which gave a good balance between low background and high signal strength (Table 9).

4.1.5. Specificity assay optimization

Another optimization that we needed to do was to identify the amount of nYghJ and YghJ needed to neutralize relevant antibodies during the pre-incubation step in our specificity assay. We should preferably add a surplus amount of protein, sufficient to decrease the response to background levels, but without wasting too much protein.

a.	Pre-incubation amount	Buffer			Buffer		
		Equivalent			Equivalent		
	Antibody levels	anti-nYghJ			anti-gYghJ		
	EV06 day 10	17862			15527		
	EV09 day 10	25217			25097		
b.	Pre-incubation amount	nYghJ protein					
		1 µg	0.5 µg	0.25 µg	1 µg	0.5 µg	0.25 µg
	Antibody levels	anti-nYghJ			anti-gYghJ		
	EV06 day 10	552	880	869	1004	1295	1206
	EV09 day 10	1127	1121	1718	6363	5983	7111
c.	Pre-incubation amount	gYghJ protein					
		1 µg	0.5 µg	0.25 µg	1 µg	0.5 µg	0.25 µg
	Antibody levels	anti-nYghJ			anti-gYghJ		
	EV06 day 10	556	796	14516	352	550	12296
	EV09 day 10	849	1121	28478	1860	2946	27806
d.	Pre-incubation amount	nYghJ and gYghJ proteins					
		1 µg	0.5 µg	0.25 µg	1 µg	0.5 µg	0.25 µg
	Antibody levels	anti-nYghJ			anti-gYghJ		
	EV06 day 10	608	507	540	528	488	535
	EV09 day 10	634	864	1159	1345	2734	4228

Table 10. Representative data from specificity assay tests performed on lavage samples. The protein levels are given as MFI values. Table 10 a. Shows pre-incubation of lavage day 10 samples with buffer, representing non-depleted antibody levels. Table 10 b and c. Show pre-incubation of lavage samples with nYghJ and gYghJ proteins, and non-glycosylated antibody-depleted and glycosylated antibody-depleted levels, respectively. Table 10 d. Show responses when lavage samples were pre-incubated with both antigens simultaneously.

For these tests, we selected two day 10 lavage samples that had the highest anti-gYghJ-specific IgA levels, diluted 25 µl of them 1:1 with 2X assay buffer, and pre-incubated them with 0.25 µg, 0.5 µg, 1 µg, and 2 µg of nYghJ and/or gYghJ (Table 10 a, b, and c). We aimed to identify the minimum amount of protein needed to reduce the signal to a minimum. In some of these tests, we added both nYghJ and gYghJ (Table 10 d) to confirm that the antibody levels could not be brought further down by adding both proteins. We found that we needed to add 1 µg of protein to

consistently neutralize anti-YghJ IgA antibodies in these samples, including in serum, so we ended up using 1 μg in our specificity assays.

4.1.6. Bead stability

The use of a linker to attach YghJ proteins to the beads increased our concerns of decay of beads over time and subsequently decreased signals.

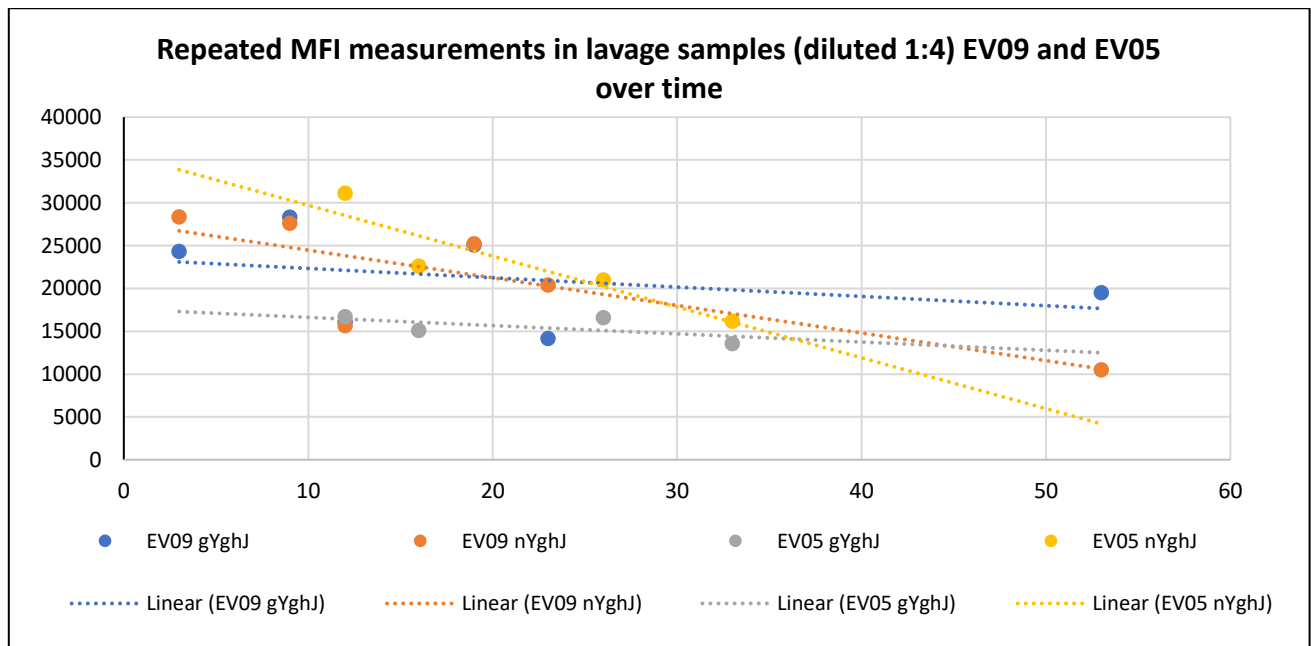


Figure 8. This figure shows the performance of the beads when samples are tested repeatedly over a period of 2 months, based on the same batch of beads. Antibody levels are given in MFI.

Therefore, to monitor the efficacy of our beads over time, a few samples both at day 0 and day 10 were repeatedly run over the entire duration of experiments to see if there was a substantial decay of bead signal (Figure 8). We noticed that there was variability and some decay over time, but not as pronounced as feared.

4.1.7. Other considerations

The lavage samples contain lower levels of antibodies than serum, and therefore we need to use larger amounts of lavage than serum in our assays (1:4 dilutions for lavage, and 1:50 for serum). Since the lavage is largely unbuffered, the lavage was first diluted in 2X assay buffer instead of assay buffer, and then again mixed with beads in 1x assay buffer to obtain a final dilution of 1:4.

The dilution of Alexa fluor® 488 was optimised for both serum and lavage to prevent overestimation of signal and to minimize background signal.

The number of each bead type added in the assay was adjusted so that 400 to 1000 beads were analysed in the flow cytometer in each well.

To be more specific about the measurement of the gut immune response, we tried several clones of alleged anti-SIgA antibodies specific for the secretory component (ECM-1/Secretory Component P85 Antibody (SC05), Novus Biologicals, Canada; Anti-IgA Secretory Component antibody [SPM217], Abcam, UK; Mouse anti-Human secretory component (free and bound) Secondary Antibody, MyBiosource, U.S.A) and none of them worked in our assay (Results not shown). However, we only tried commercial fluorochrome-conjugated versions of these antibodies, as we wanted to avoid a tertiary antibody in our assay.

4.2. Strengths of the study

A strength of this study is our use of arbitrary units instead of MFI values, which is normally done, as measures of antibody levels in our samples. We believe this has resulted in more accurate results. Similarly, we also adjusted for total IgA levels in our lavage samples to compensate for

between-sample variation in IgA levels in our analyses, again most likely improving the accuracy of our results.

The ability to multiplex our assays is another strength. This simplifies comparison between multiplexed assays and reduces the amounts of samples needed for the assays. Once optimized, these methods are less time-consuming to undertake and likely to be more accurate than alternative immunoassay techniques such as ELISA.

During the course of optimization, a few of the samples were run repeatedly at different times, and the results remained largely the same (as indicated in Figure 8), suggesting that results from these assays are reproducible.

Our assays only require small amounts of reagents (e.g., only around 80 µg of protein and 8 million beads could analyse more than 400 samples), and the assays could easily be expanded if additional assays were needed, including testing for anti-YghJ IgG or IgM antibodies, or testing other YghJ variants.

The specificity assay we developed can also be useful in estimating proportions of antibodies that target glycosylated epitopes in other proteins.

4.3. Limitations of the study

Direct comparisons of antibody level estimates obtained for different types of YghJ cannot be made since there are always inherent differences in the actual amounts and quality of the YghJ bound to the beads. Even after we had normalized the lavage sample results, there seemed to be a much larger variation in anti-YghJ antibody levels in lavage than in the blood samples. We believe these findings are accurate, but this uncertainty could be addressed by analysing circulating B-

cells in antibody in lymphocyte supernatant (ALS) samples. ALS levels should correlate well with the gut antibody levels (36).

Our sample size of 21 samples was rather small, while variability in the assays was quite large, especially for lavage samples. Increasing the number of volunteers would have given us more accurate estimates, particularly for our specificity assays.

Finally, although the samples we have used in this study are unique, the immune responses of adults who are immunologically naïve to ETEC infections may not necessarily reflect the immune responses of the population who are the targets for vaccination, including LMIC children. So, the results generated in this study may not readily be generalizable.

4.4. Conclusions

YghJ is a virulence factor produced by ca. 89 % of pathogenic *E. coli* isolates, it has the ability to degrade major mucins and facilitate the delivery of LT to the epithelial cells (55), and it is consistently recognised by the immune system during an infection. These are all good attributes that make YghJ a potentially good vaccine target.

In our study, we have successfully shown that IgA antibody responses to YghJ often also target glycosylated epitopes. Our findings suggest a connection between YghJ glycosylation and activation of additional antibody specificities that cannot be triggered by vaccines based on non-glycosylated YghJ.

4.5. Future Aspects

Pathogenic *E. coli* represent a phenotypically diverse group of pathogens with few conserved virulence factors (55) that are promising vaccine candidates. Further studies to evaluate if these glycosylation targeting antibodies can offer cross-protection against the mucinase activity of YghJ from other strains of *E. coli* will contribute to the development of YghJ-based vaccines. Therefore, it would be of interest to ascertain if the antibodies elicited against the glycosylated YghJ can reduce the mucinase activity of YghJ from TW10722 as well as YghJ from other pathogenic *E. coli* in functional assays.

Further research is also warranted to test if the pattern of glycosylation is exclusive for each strain or is it shared between different ETEC strains. Similarly, assays can also be designed to see if the non-glycosylated antigen is pathologically different than the non-glycosylated antigens in its function.

Finally, YghJ protein is secreted by many commensal as well as pathogenic strains of *E. coli* (59) and we are not aware of the consequences of targeting the gut commensals or their ability to secrete YghJ. Therefore, the question of how glycosylated YghJ can be safely be targeted by vaccines in a way that does not disrupt gut microflora is yet to be addressed (20, 55).

REFERENCES

1. Riaz S, Steinsland H, Hanevik K. Human Mucosal IgA Immune Responses against Enterotoxigenic *Escherichia coli*. *Pathogens*. 2020;9(9).
2. Denamur E, Clermont O, Bonacorsi S, Gordon D. The population genetics of pathogenic *Escherichia coli*. *Nat Rev Microbiol*. 2020.
3. Russo TA, Johnson JR. Proposal for a new inclusive designation for extraintestinal pathogenic isolates of *Escherichia coli*: ExPEC. *J Infect Dis*. 2000;181(5):1753-4.
4. Nguyen RN, Taylor LS, Tauschek M, Robins-Browne RM. Atypical enteropathogenic *Escherichia coli* infection and prolonged diarrhea in children. *Emerg Infect Dis*. 2006;12(4):597-603.
5. Chandran A, Mazumder A. Pathogenic potential, genetic diversity, and population structure of *Escherichia coli* strains isolated from a forest-dominated watershed (Comox Lake) in British Columbia, Canada. *Appl Environ Microbiol*. 2015;81(5):1788-98.
6. Sack RB, Gorbach SL, Banwell JG, Jacobs B, Chatterjee BD, Mitra RC. Enterotoxigenic *Escherichia coli* isolated from patients with severe cholera-like disease. *J Infect Dis*. 1971;123(4):378-85.
7. Coimbra RS, Grimont F, Lenormand P, Burguiere P, Beutin L, Grimont PA. Identification of *Escherichia coli* O-serogroups by restriction of the amplified O-antigen gene cluster (*rfb-RFLP*). *Res Microbiol*. 2000;151(8):639-54.
8. Tacket CO, Losonsky G, Link H, Hoang Y, Guesry P, Hilpert H, et al. Protection by milk immunoglobulin concentrate against oral challenge with enterotoxigenic *Escherichia coli*. *N Engl J Med*. 1988;318(19):1240-3.
9. Levine MM, Ristaino P, Marley G, Smyth C, Knutton S, Boedeker E, et al. Coli surface antigens 1 and 3 of colonization factor antigen II-positive enterotoxigenic *Escherichia coli*: morphology, purification, and immune responses in humans. *Infection and Immunity*. 1984;44(2):409-20.
10. Del Canto F, O'Ryan M, Pardo M, Torres A, Gutiérrez D, Cádiz L, et al. Chaperone-Usher Pili Loci of Colonization Factor-Negative Human Enterotoxigenic *Escherichia coli*. *Frontiers in Cellular and Infection Microbiology*. 2017;6(200).
11. Del Canto F, Valenzuela P, Cantero L, Bronstein J, Blanco JE, Blanco J, et al. Distribution of classical and nonclassical virulence genes in enterotoxigenic *Escherichia coli* isolates from Chilean children and tRNA gene screening for putative insertion sites for genomic islands. *J Clin Microbiol*. 2011;49(9):3198-203.
12. Zeinalzadeh N, Salmanian AH, Ahangari G, Sadeghi M, Amani J, Bathaie SZ, et al. Design and characterization of a chimeric multiepitope construct containing CfaB, heat-stable toxin, CstA, CstB, and heat-labile toxin subunit B of enterotoxigenic *Escherichia coli*: a bioinformatic approach. *Biotechnol Appl Biochem*. 2014;61(5):517-27.
13. Norton EB, Branco LM, Clements JD. Evaluating the A-Subunit of the Heat-Labile Toxin (LT) As an Immunogen and a Protective Antigen Against Enterotoxigenic *Escherichia coli* (ETEC). *PLoS One*. 2015;10(8):e0136302.
14. Joffré E, Sjöling Å. The LT1 and LT2 variants of the enterotoxigenic *Escherichia coli* (ETEC) heat-labile toxin (LT) are associated with major ETEC lineages. *Gut Microbes*. 2016;7(1):75-81.
15. Sakkestad ST, Steinsland H, Skrede S, Lillebo K, Skutlaberg DH, Guttormsen AB, et al. A new human challenge model for testing heat-stable toxin-based vaccine candidates for enterotoxigenic *Escherichia coli* diarrhea - dose optimization, clinical outcomes, and CD4+ T cell responses. *PLoS Negl Trop Dis*. 2019;13(10):e0007823.
16. Nesta B, Valeri M, Spagnuolo A, Rosini R, Mora M, Donato P, et al. SsIE elicits functional antibodies that impair in vitro mucinase activity and in vivo colonization by both intestinal and extraintestinal *Escherichia coli* strains. *PLoS Pathog*. 2014;10(5):e1004124.

17. Luo Q, Kumar P, Vickers TJ, Sheikh A, Lewis WG, Rasko DA, et al. Enterotoxigenic *Escherichia coli* secretes a highly conserved mucin-degrading metalloprotease to effectively engage intestinal epithelial cells. *Infect Immun*. 2014;82(2):509-21.
18. Strozen TG, Li G, Howard SP. YghG Is a Novel Pilot Protein Required for Localization of the GspS Type II Secretion System Secretin of Enterotoxigenic *Escherichia coli*. *Infection and Immunity*. 2012;80(8):2608-22.
19. Chakraborty S, Randall A, Vickers TJ, Molina D, Harro CD, DeNearing B, et al. Human Experimental Challenge With Enterotoxigenic *Escherichia coli* Elicits Immune Responses to Canonical and Novel Antigens Relevant to Vaccine Development. *J Infect Dis*. 2018;218(9):1436-46.
20. Mirhoseini A, Amani J, Nazarian S. Review on pathogenicity mechanism of enterotoxigenic *Escherichia coli* and vaccines against it. *Microb Pathog*. 2018;117:162-9.
21. Boysen A, Palmisano G, Krogh TJ, Duggin IG, Larsen MR, Moller-Jensen J. A novel mass spectrometric strategy "BEMAP" reveals Extensive O-linked protein glycosylation in Enterotoxigenic *Escherichia coli*. *Sci Rep*. 2016;6:32016.
22. Rachmilewitz J. Glycosylation: An intrinsic sign of "danger". *Self Nonself*. 2010;1(3):250-4.
23. Lisowska E. The role of glycosylation in protein antigenic properties. *Cell Mol Life Sci*. 2002;59(3):445-55.
24. Lithgow KV, Scott NE, Iwashkiw JA, Thomson EL, Foster LJ, Feldman MF, et al. A general protein O-glycosylation system within the Burkholderia cepacia complex is involved in motility and virulence. *Mol Microbiol*. 2014;92(1):116-37.
25. Thaïss CA, Zmora N, Levy M, Elinav E. The microbiome and innate immunity. *Nature*. 2016;535(7610):65-74.
26. Hoces D, Arnoldini M, Diard M, Loverdo C, Slack E. Growing, evolving and sticking in a flowing environment: understanding IgA interactions with bacteria in the gut. *Immunology*. 2020;159(1):52-62.
27. Masahata K, Umemoto E, Kayama H, Kotani M, Nakamura S, Kurakawa T, et al. Generation of colonic IgA-secreting cells in the caecal patch. *Nat Commun*. 2014;5:3704.
28. Mora JR, Iwata M, Eksteen B, Song SY, Junt T, Senman B, et al. Generation of gut-homing IgA-secreting B cells by intestinal dendritic cells. *Science*. 2006;314(5802):1157-60.
29. Kantele A. Antibody-secreting cells in the evaluation of the immunogenicity of an oral vaccine. *Vaccine*. 1990;8(4):321-6.
30. Yang Y, Palm NW. Immunoglobulin A and the microbiome. *Curr Opin Microbiol*. 2020;56:89-96.
31. Macpherson AJ, McCoy KD, Johansen FE, Brandtzaeg P. The immune geography of IgA induction and function. *Mucosal Immunol*. 2008;1(1):11-22.
32. Chakraborty S, Harro C, DeNearing B, Ram M, Feller A, Cage A, et al. Characterization of Mucosal Immune Responses to Enterotoxigenic *Escherichia coli* Vaccine Antigens in a Human Challenge Model: Response Profiles after Primary Infection and Homologous Rechallenge with Strain H10407. *Clin Vaccine Immunol*. 2016;23(1):55-64.
33. Qadri F, Ahmed T, Ahmed F, Bhuiyan MS, Mostofa MG, Cassels FJ, et al. Mucosal and systemic immune responses in patients with diarrhea due to CS6-expressing enterotoxigenic *Escherichia coli*. *Infect Immun*. 2007;75(5):2269-74.
34. Brandtzaeg P. Induction of secretory immunity and memory at mucosal surfaces. *Vaccine*. 2007;25(30):5467-84.
35. Spencer J, Sollid LM. The human intestinal B-cell response. *Mucosal Immunol*. 2016;9(5):1113-24.
36. Aase A, Sommerfelt H, Petersen LB, Bolstad M, Cox RJ, Langeland N, et al. Salivary IgA from the sublingual compartment as a novel noninvasive proxy for intestinal immune induction. *Mucosal Immunology*. 2016;9(4):884-93.

37. He B, Xu W, Santini PA, Polydorides AD, Chiu A, Estrella J, et al. Intestinal bacteria trigger T cell-independent immunoglobulin A(2) class switching by inducing epithelial-cell secretion of the cytokine APRIL. *Immunity*. 2007;26(6):812-26.
38. Corthesy B. Multi-faceted functions of secretory IgA at mucosal surfaces. *Front Immunol*. 2013;4:185.
39. Moor K, Diard M, Sellin ME, Felmy B, Wotzka SY, Toska A, et al. High-avidity IgA protects the intestine by enchainning growing bacteria. *Nature*. 2017;544(7651):498-502.
40. Brandtzaeg P. The mucosal immune system and its integration with the mammary glands. *J Pediatr*. 2010;156(2 Suppl):S8-15.
41. Boschi-Pinto C, Velebit L, Shibuya K. Estimating child mortality due to diarrhoea in developing countries. *Bull World Health Organ*. 2008;86(9):710-7.
42. Troeger C, Colombara DV, Rao PC, Khalil IA, Brown A, Brewer TG, et al. Global disability-adjusted life-year estimates of long-term health burden and undernutrition attributable to diarrhoeal diseases in children younger than 5 years. *Lancet Glob Health*. 2018;6(3):e255-e69.
43. Kotloff KL, Nataro JP, Blackwelder WC, Nasrin D, Farag TH, Panchalingam S, et al. Burden and aetiology of diarrhoeal disease in infants and young children in developing countries (the Global Enteric Multicenter Study, GEMS): a prospective, case-control study. *Lancet*. 2013;382(9888):209-22.
44. Khalil IA, Troeger C, Blacker BF, Rao PC, Brown A, Atherly DE, et al. Morbidity and mortality due to shigella and enterotoxigenic *Escherichia coli* diarrhoea: the Global Burden of Disease Study 1990-2016. *Lancet Infect Dis*. 2018;18(11):1229-40.
45. Radlovic N, Lekovic Z, Vuletic B, Radlovic V, Simic D. Acute Diarrhea in Children. *Srp Arh Celok Lek*. 2015;143(11-12):755-62.
46. Gilmartin AA, Petri WA, Jr. Exploring the role of environmental enteropathy in malnutrition, infant development and oral vaccine response. *Philos Trans R Soc Lond B Biol Sci*. 2015;370(1671).
47. Pinkerton R, Oria RB, Lima AA, Rogawski ET, Oria MO, Patrick PD, et al. Early Childhood Diarrhea Predicts Cognitive Delays in Later Childhood Independently of Malnutrition. *Am J Trop Med Hyg*. 2016;95(5):1004-10.
48. DuPont HL. Persistent Diarrhea: A Clinical Review. *JAMA*. 2016;315(24):2712-23.
49. Fink G, D'Acromont V, Leslie HH, Cohen J. Antibiotic exposure among children younger than 5 years in low-income and middle-income countries: a cross-sectional study of nationally representative facility-based and household-based surveys. *Lancet Infect Dis*. 2020;20(2):179-87.
50. <PPC_ETEC_April_2020_Public_Consultation.pdf>.
51. Levine MM, Nalin DR, Hoover DL, Bergquist EJ, Hornick RB, Young CR. Immunity to enterotoxigenic *Escherichia coli*. *Infect Immun*. 1979;23(3):729-36.
52. Chakraborty S, Randall A, Vickers TJ, Molina D, Harro CD, DeNearing B, et al. Interrogation of a live-attenuated enterotoxigenic *Escherichia coli* vaccine highlights features unique to wild-type infection. *NPJ Vaccines*. 2019;4:37.
53. Avci FY, Kasper DL. How bacterial carbohydrates influence the adaptive immune system. *Annu Rev Immunol*. 2010;28:107-30.
54. Todnem Sakkestad S, Steinsland H, Skrede S, Kleppa E, Lillebo K, Saevik M, et al. Experimental Infection of Human Volunteers with the Heat-Stable Enterotoxin-Producing Enterotoxigenic *Escherichia coli* Strain TW11681. *Pathogens*. 2019;8(2).
55. Luo Q, Qadri F, Kansal R, Rasko DA, Sheikh A, Fleckenstein JM. Conservation and immunogenicity of novel antigens in diverse isolates of enterotoxigenic *Escherichia coli*. *PLoS Negl Trop Dis*. 2015;9(1):e0003446.
56. Skrede S, Steinsland H, Sommerfelt H, Aase A, Brandtzaeg P, Langeland N, et al. Experimental infection of healthy volunteers with enterotoxigenic *Escherichia coli* wild-type strain TW10598 in a hospital ward. *BMC Infect Dis*. 2014;14:482.

57. Adan A, Alizada G, Kiraz Y, Baran Y, Nalbant A. Flow cytometry: basic principles and applications. *Crit Rev Biotechnol.* 2017;37(2):163-76.
58. Ondigo BN, Park GS, Gose SO, Ho BM, Ochola LA, Ayodo GO, et al. Standardization and validation of a cytometric bead assay to assess antibodies to multiple *Plasmodium falciparum* recombinant antigens. *Malar J.* 2012;11:427.
59. Tapader R, Bose D, Pal A. YghJ, the secreted metalloprotease of pathogenic *E. coli* induces hemorrhagic fluid accumulation in mouse ileal loop. *Microb Pathog.* 2017;105:96-9.

APPENDIX

A. Guidelines from the journal

We plan to submit our manuscript in Infection and Immunity Journal (IAI) by American Society for Microbiology (ASM). The journal is format-neutral for initial submission of manuscript. However, we have adopted the standard Introduction – Method – Results – and – Discussion (IMRaD) format for structure of the manuscript. For references, we have used Vancouver reference style.

B. Ethical approval

The project is registered under Helse Bergen. The study was approved by the Regional Committee for Medical and Health Research Ethics, Health Region West (REC-West; case number 2010/728-14). The volunteers signed written informed consent to participate in the study and could leave at any point at will. The study was monitored by an independent monitor.

Human systemic and intestinal IgA responses against the mucinase YghJ following experimental infection with enterotoxigenic *Escherichia coli*

Saman Riaz^{1,2}, Hans Steinsland^{3,4}, Mette Thorsing⁵, Ann Z. Andersen⁵, Anders Boysen⁵, Kurt Hanevik^{1,6,*}

¹ Department of Clinical Science, University of Bergen, Bergen, Norway

² Centre for International Health, Department of Global Public Health and Primary Care, University of Bergen, Bergen, Norway

³ Centre for Intervention Science in Maternal and Child Health (CISMAC), Centre for International Health, Department of Global Public Health and Primary Care, University of Bergen, Bergen, Norway

⁴ Department of Biomedicine, University of Bergen, Bergen, Norway

⁵ GlyProVac ApS, Odense, Denmark

⁶ Norwegian National Advisory Unit on Tropical Infectious Diseases, Department of Medicine, Haukeland University Hospital, Bergen, Norway

* Correspondence: Kurt.Hanevik@uib.no; Tel.: +47 5597 5000; Fax: +47 5597 2950

Keywords

Enterotoxigenic *Escherichia coli*, immunogenicity, vaccine development, protein glycosylation, IgA, SsIE

Word count: 5465 (including figures and tables)

Abstract word count: 300

ABSTRACT

Enterotoxigenic *Escherichia coli* (ETEC) is an important cause of diarrheal disease in young children in middle- and low-income countries and in travelers to these countries. Efforts are ongoing to develop broadly protective vaccines against these pathogens. One of the targets for vaccine development is the metalloprotease YghJ, which is a conserved mucinase that is immunogenic and produced by most pathogenic *E. coli*. Recent studies have shown that YghJ is heavily glycosylated, but it is unclear how glycosylation affect the immune responses targeting YghJ.

In this study we found that 64 amino acid residues of the 170 kDa YghJ protein from ETEC strain TW10722 were O-glycosylated. To evaluate antibody responses targeting YghJ and its glycosylated epitopes, we analysed serum and intestinal lavage samples from 21 volunteers who had been experimentally infected with ETEC TW10722. By comparing IgA responses between before and 10 days after ingesting the ETEC strain in a multiplex bead flow cytometric assay based on glycosylated and non-glycosylated YghJ, we found that the median proportion of anti-YghJ IgA that specifically targeted glycosylated epitopes was 0.54 (IQR: 0.32, 0.90) in serum and 0.07 (IQR: 0.01, 0.22) in the lavage samples. The overall fold increase in IgA antibodies against glycosylated YghJ was median 7.9 (IQR: 7.1, 11.1) in serum and 3.7 (IQR: 2.0, 10.7) in lavage, with 20 (95%) volunteers having responded to glycosylated YghJ (≥ 2 -fold IgA increase in serum). Responses did not seem to be associated with diarrhea. Our findings suggest that a substantial, but variable, proportion of the IgA antibody response to YghJ in serum during an ETEC infection was targeted against glycosylated epitopes, but that gut IgA responses largely targeted non-glycosylated epitopes. While these results need further investigation, they indicate that glycosylation of vaccine antigens could play an important role in creating protective immunity against ETEC infection.

INTRODUCTION

Enterotoxigenic *Escherichia coli* (ETEC) causes around 75 million episodes of diarrhea and 50,000 deaths among children less than 5 years of age in low- and middle-income countries (LMICs) each year (1). In addition, infection with ETEC is often the cause of diarrhea among adults traveling to endemic countries for employment or recreational purposes. Improved rehydration therapy and sanitary conditions have caused a decline in the mortality rate of diarrheal diseases, but not in morbidity (2).

The effort to develop vaccines against pathogenic *E. coli* has been ongoing for several decades (3), and several different protein virulence factors are currently being evaluated for use in vaccines against these pathogens (4, 5). One of the relatively newly discovered virulence factors is YghJ, which is a large metalloprotease secreted by most pathogenic *E. coli* (6, 7). YghJ assists in breaking down the MUC2 and MUC3 proteins in the mucosal layers of the gut so that the *E. coli* can reach the intestinal cell wall (8). YghJ is secreted by the same type 2 secretion system (T2SS) that is also implicated in the secretion of the ETEC heat-stable toxin (LT). It is believed that YghJ helps deliver LT to the epithelial cells (8-10), thus playing an integral role in both colonization and development of diarrhoea. In animal experiments, pre-treatment with anti-YghJ antibodies resulted in decreased mucinase activity and impaired colonization with pathogenic *E. coli* (11), and human volunteers experimentally infected with wild-type ETEC often develop strong anti-YghJ IgA responses both when measured in serum and in antibodies in lymphocyte supernatants (ALS) (12-14).

Attachment of a sugar molecule to the oxygen atom of serine (Ser) or threonine (Thr) amino acids in a protein is called O-linked glycosylation. In bacteria, it occurs in the cytoplasm at the post-translational level (15). Until recently this type of post translational modification (PTM) has been viewed as rare, and as such only a small number of *E. coli* glycosylated

proteins have been identified and characterized (16-18). However, with the emergence of new methods to investigate bacterial O-linked glycosylation, this PTM appears to be widespread across the *E. coli* population (15). The presence of O-linked glycosylation changes the proteins' phenotypic properties, and could, for example, affect the pathogen's ability to adhere to, colonize, or penetrate the host tissue (19, 20). Previous studies have also shown that glycosylation contributes to the pathogen's or its virulence factors' abilities to evade immune responses (21-23). *E. coli* glycosylates many of its cell surface proteins, and the presence of glycosylation is usually more pronounced in pathogenic compared to commensal *E. coli* (20). The fact that most proteins associated with the cell surface, or with outer membrane vesicles of pathogenic *E. coli*, are heavily O-glycosylated, including the secreted YghJ, indicate an association with pathogenicity (20).

Natural and experimental ETEC infections appear to consistently generate strong and similar immune responses against YghJ, both cell- and antibody-mediated, as measured in serum (6, 12, 13).

Studies of HIV-1 gp120 protein have shown the importance of the selection of an appropriately glycosylated HIV-1 envelope as a vaccine antigen (24). Romain *et al.* (25) furthermore found that de-glycosylation of antigens used for immunization often gives a substantially poorer T lymphocyte response, again suggesting that subunit vaccines may benefit from using native, glycosylated vaccine antigens. For ETEC, native virulence factors appear to induce stronger immune responses than recombinant or denatured proteins given as vaccines (5).

To further the effort to develop YghJ-based vaccines, we wanted to evaluate whether human experimental ETEC infection may induce anti-YghJ IgA responses in the gut similar to what has been observed in serum (12, 13), and to evaluate how much of the YghJ-specific IgA

antibodies in the gut and serum actually target glycosylated epitopes on YghJ. To achieve this, we developed and used a multiplex bead-based flow cytometric immunoassay to estimate anti-YghJ IgA responses in human intestinal lavage samples and serum, and selectively neutralized antibodies targeting non-glycosylated YghJ epitopes to estimate the proportion of anti-YghJ IgA that specifically targeted glycosylated epitopes. We also assessed whether these characteristics were associated with the development of diarrhoea from the infection.

MATERIALS AND METHODS

Experimental ETEC infection study

Details of the experimental ETEC infection study have been described earlier by Sakkestad *et al.* (13). Briefly, 21 healthy adult volunteers aged between 18 and 40 years, who were presumed to be immunologically naïve to ETEC, were experimentally infected with ETEC strain TW10722 by ingesting doses ranging from 1×10^6 to 1×10^{10} colony forming units (CFU). The infection was cleared 5 days after dose ingestion, or within 24 hours of experiencing severe symptoms, by treatment with ciprofloxacin. The volunteers were considered to have diarrhea if they passed 1 loose or liquid stool weighing ≥ 300 g, or ≥ 2 loose or liquid stools combinedly weighing ≥ 200 g during any 48-hour period within 120 hours after dose ingestion. Ten of the 21 volunteers developed diarrhoea (13).

ETEC strain TW10722 (O115:H5; GenBank BioProject: PRJNA59745) was isolated in 1997 in Guinea-Bissau from a 15-month-old child who was suffering from acute diarrhoea. The strain encodes the two ETEC colonization factors coli surface antigen 5 (CS5) and CS6. It also encodes the human variant of the heat-stable enterotoxin (STh), but not the heat-labile toxin (LT).

Specimen collection and preparation

In the present study, we use serum samples from these 21 volunteers collected on the day of dose ingestion and 10 days after, as well as intestinal lavage samples collected a few weeks before dose ingestion and 10 days after.

To obtain intestinal lavage specimens, the volunteers drank a polyethylene glycol-based laxative (Laxabon; Karo Pharma AB, Stockholm, Sweden) until the stools were clear and watery. After mixing with EDTA-free cOmplete Protease Inhibitor Cocktail (Roche, Basel, Switzerland), samples were immediately stored at -70°C until the experimental infection study had ended. For the current analyses, aliquots of these lavage specimens were thawed on ice, centrifuged at $16,000 \times g$ for 3 min, and the supernatant was subsequently filtered successively through 1 μm , 0.45 μm , and 0.22 μm pore size syringe filters before being stored at -70°C until use.

Glycosylated YghJ production

To obtain glycosylated YghJ from TW10722 a DNA sequence encoding the 3xFLAG peptide was inserted immediately after *yghJ* on the TW10722 chromosome. This enables the purification of native YghJ from TW10722 by using 3xFLAG-specific antibody capture methods. Based on the recombinational tagging protocol described by Uzzau *et al.* (26), a PCR product was generated by using the 3xFLAG sequence and kanamycin resistance gene in pSUB11 as a template and the primer pair GPV128+GPV129 (Table 1). After purification, the PCR product was electroporated into TW10722 by using a Bio-Rad gene pulser (pulse parameters: 1.80 kV, 25 μF , and 200Ω). Transformants were selected on Luria Bertani (LB) agar plates containing 40 $\mu\text{g/ml}$ kanamycin. Sanger sequencing-based on primer pairs

GPV127+GPV17 and GPV67+GPV147 (Table 1) were used to verify that the 3xFLAG sequence was correctly inserted.

To purify glycosylated YghJ from this modified TW10722 strain, the strain was grown in M9 minimal medium (27) supplemented with 0.2% glucose, 0.4% casamino acid, and 40 µg/ml kanamycin. The culture was grown at 37°C to an OD₆₀₀ of 2.5 before harvesting the YghJ-containing supernatant by centrifugation at 15,250 × g at 2°C for 20 min. The supernatant was sterile filtered (0.22 µm pore size) before NaCl and Triton X-100 were added to 200 mM and 0.01% final concentrations, respectively. ANTI-FLAG M2 Affinity Gel (Product no.: A2220; Sigma-Aldrich, St. Louis, MO) agarose beads were added to the supernatant and incubated shaken overnight at 4°C. After sterile filtration, the recovered beads were washed twice with FLAG Sup wash buffer I (phosphate buffered saline [PBS], pH 7.6, containing 400 mM NaCl, 0.1% Triton X-100, and 1 mM EDTA) and once with FLAG Sup buffer II (PBS, pH 7.6, containing 400 mM NaCl, 0.01% Triton X-100, and 1 mM EDTA). The glycosylated YghJ was eluted by incubating in Elution buffer (500 mM arginine, 500 mM NaCl, pH 3.5), after which 1 M Tris base was added until the pH reached 7.6. Eluates were spin filter concentrated before overnight dialysis at 4°C against PBS, pH 7.6, containing 0.1% Triton X-100, which helps to keep the glycosylated YghJ in solution.

Table 1. Sequences of DNA primers used for cloning and testing YghJ constructs.

Primers	Sequence	Comment
GPV17	AGCAGCGGAATATTGTCACGTAT	yghJ rv
GPV67	GAAGGAATGGGCAGAGAAAAACT	yghJ fw segment 7
GPV127	TCGTTAATATCATCCGGCTTCAT	yghJ fw
GPV128	AAGCTGCCGAAACCGGAACAGGGACCGGAAACCATTA CAAGGTTACCGAGCATAAGATGTCTGTCGAG	yghJ 3xFLAG fw

	<i>GACTACAAAGACCATGACGG</i>	
GPV129	TAAGCTGGCGCAACCCGGTGC GCCTTATTTTCATGCCGGA TGCGGCGTGAACGCCTTATCCGGCATAACAGGA <i>CATATGAATATCCTCCTTAG</i>	yghJ 3xFLAG rv
GPV130	ACTTAGATTC AATTGTGAGC <u>CACCATAAGGAGTTTTATAA</u> atgAATAAGAAATTTAAATA TAAGA	ETEC TW10722 IPTG SD yghJ fw1
GPV131	TAGCTACTCGAGGGCAAAAAGAGTGTGACTTGTGAGCG GATAACAATGATACTTAGATTC AATTGTGAGC <u>CACCAT</u>	ETEC TW10722 IPTG SD yghJ fw2
GPV132	TATCATGATCTTTATAATCACCGTCATGGTCTTTGTAGTC CTCGACAGACATCTTATGCTCGGTAAC	ETEC TW10722 yghJ FLAG rv1
GPV133	TAGCTATCTAGATTACTATTTATCGTCGTCATCTTTGTAG TCGATATCATGATCTTTATAATCACCGTCAT	ETEC TW10722 yghJ FLAG rv2
GPV 97	TAGCTAGC TCTAG TTAGTATTTATCGTCGTCATCTTTG	FLAG rv
GPV147	CAGTCATAGCCGAATAGCCT	K1 oligo, Wanner

Non-glycosylated YghJ production

To produce non-glycosylated YghJ, we cloned *yghJ* and the appended 3xFLAG sequence generated above into an expression vector and produced it recombinantly in an *E. coli* MG1655 strain that had a non-functioning *hldE*. HldE is responsible for synthesizing the heptose glycans that *E. coli* use for protein glycosylation (28). We first amplified the *yghJ* sequence and 3xFLAG sequence from the modified TW10722 described above by using primer pairs GPV130+GPV132. This PCR product was then further amplified by using primer pairs GPV131+GPV133 to generate a product that was digested with XhoI and XbaI and subsequently ligated into the expression vector pXG-0 (29), creating pGPV106. Before

transforming pGV106 into *E. coli* MG1655 Δ hldE, we sequenced it to ensure that *yghJ* and the 3xFLAG sequence were correctly inserted.

To produce the non-glycosylated YghJ, this strain was grown at 37°C in 10 L LB medium supplemented with 40 μ g/ml chloramphenicol and 1 mM isopropyl- β -D-1-thiogalactopyranoside (IPTG) until reaching an OD₆₀₀ of 2.5, before harvesting the YghJ-containing cells by centrifugation at 15,250 \times g, 2°C for 15 min. Cell pellets were resuspended in PBS, pH 7.6, containing 500 μ g DNase I before being passed three times through a French Press at 2.2 kbar. The resulting lysate was cleared by ultracentrifugation at 125,000 \times g at 4°C for three hours in a swinging-bucket rotor before diluting the resulting supernatant to 1 L with PBS, pH 7.6, with NaCl, Triton X-100, and EDTA added to final concentrations of 600 mM, 0.01%, and 1 mM, respectively. The non-glycosylated YghJ was then purified, concentrated, and dialyzed as described above for the glycosylated YghJ production, with the exception that the FLAG Lys wash buffer I and II contained 600 mM instead of 400 mM NaCl.

Protein testing

The purified proteins were quantified by using the BCA Micro assay (Thermo Fisher Scientific, Waltham, MA). We confirmed that the purified proteins contained YghJ by performing native and denaturing western blotting. In these assays, 50 ng native or denatured YghJ proteins were separated on NuPAGE 4 to 12% gradient Bis-Tris polyacrylamide gels (Thermo Fisher Scientific) by using native PAGE or SDS-PAGE, respectively, together with the SeeBlue Plus2 Pre-stained Standard (Thermo Fisher Scientific) molecular weight marker, before being transferred to a polyvinylidene difluoride (PVDF) membrane. To obtain a clear separation of YghJ in the native PAGE, we mixed the protein in 1x SDS native loading buffer (60 mM Tris-Cl, pH 6.8, 10% glycerol, 0.005% bromophenol blue) and used an MES-based

running buffer that contained small amounts of SDS (50 mM MES, 50 mM Tris-base, 0.01% SDS, pH 7.3). We found that the addition of 0.01% SDS greatly improved the band resolution in these assays.

To detect FLAG-tagged YghJ, the membranes were incubated in PBS containing 1% skimmed milk powder and 0.05% Tween-20 as follows: 1 hour without any additives, 1 hour with monoclonal anti-FLAG M2 mouse antibodies (Product no.: F3165; Sigma-Aldrich), and 1 hour with HRP-conjugated rabbit Anti-mouse IgG (Product no.: P0260; Dako Denmark AS, Næstved, Denmark). The blot images were captured on a GE Amersham Imager 680 (GE Healthcare, Chicago, Il) after wetting with Immobilon Forte Western HRP substrate (Merck KGaA, Darmstadt, Germany). To test for YghJ-specificity, we instead incubated the membranes in PBS containing 3% skimmed milk powder and 0.05% Tween-20, added diluted volunteer serum, and used HRP-conjugated polyclonal rabbit anti-Human IgA, IgG, IgM, Kappa, Lambda antibody (Product no.: P0212; Dako Denmark AS) as the secondary antibody instead.

To evaluate the glycosylation of the native YghJ, we performed BEMAB analysis to identify glycosylated serine and threonine residues, as previously described (20).

Bead coupling

The proteins, including glycosylated YghJ (gYghJ) and non-glycosylated YghJ (nYghJ) were covalently coupled to 4 μ m Cyto-Plex carboxylated beads (Thermo Fisher Scientific, Waltham, MA) of different fluorescence levels. Since the YghJ protein solutions contained Triton X-100, which may interfere with and reduce the efficiency of coupling the proteins directly onto these polystyrene beads, we first coupled long polyethylene glycol linkers to the beads and then coupled the proteins to these linkers. Both coupling reactions were done by

using carboxyl-to-amine crosslinking chemistry based on N-(dimethylaminopropyl)-N'-ethyl carbodiimide HCl (EDC) and N-hydroxysulfosuccinimide (Sulfo-NHS).

The wells of a MultiScreen HTS filter plate (Merck KGaA) were wetted with 100 μ L MES buffer (50 mM 2-[N-morpholino] ethanesulfonic (MES) acid, pH 5.5) followed by centrifugation at $300 \times g$ for 45 sec at room temperature. All remaining centrifugations were done at a lower $50 \times g$ for 45 sec at room temperature to minimize the risk of beads sticking to the filter, and during the first wash in each step described below, we also scraped the tip of the pipet along the edges of the well-bottom during mixing to ensure complete resuspension of the beads. Approximately 8 million beads diluted in 50 μ l MES buffer were added to the wells, followed by centrifugation, wash in 200 μ l MES buffer, and centrifugation. A mix of 160 μ L MES buffer, 20 μ L MES buffer containing 50 mg/mL freshly prepared EDC, and 20 μ L MES buffer containing 50 mg/mL freshly prepared Sulfo-NHS were added and mixed with the beads. After incubating at room temperature for 20 minutes on a microplate shaker (600 rpm, 3 mm \emptyset), the beads were washed twice with 200 μ L MES buffer. We then added 200 μ l MES buffer containing 2 mg of the PEG linker (Poly[ethylene glycol] 2-aminoethyl ether acetic acid of 2.1 kDa average molecular weight [Product no. 757888-100MG; Sigma-Aldrich]) and incubated for 2 h at room temperature on a shaker, followed by three washes. To couple the proteins to the carboxylated ends of the PEG linker, we repeated the last steps above, including adding fresh EDC and Sulfo-NHS, incubating and washing, before adding 18 μ g of non-glycosylated or glycosylated YghJ. Protein concentration was determined a day in advance by using the BCA Micro assay (Thermo Fisher Scientific). After overnight incubation on a shaker at 4°C, the beads were washed twice with PBS, pH 7.4, and resuspended in 400 μ L storage buffer (PBS, pH 7.4, 1% bovine serum albumin [BSA], and 0.05% Tween-20), before the bead concentration was determined by using a Bürker counting chamber, and storage at 4°C until use.

Bead-based anti-YghJ antibody assay

In the bead-based antibody assays, we pooled beads coupled with non-glycosylated YghJ (nYghJ) and glycosylated YghJ (gYghJ). Serum samples were diluted 1:50 in assay buffer, lavage samples were diluted 1:2 in 2X assay buffer, and the secondary antibody (Alexa fluor 488 Affinipure Goat Anti-human serum IgA antibody [Jackson ImmunoResearch, West Grove, PA]) was diluted 1:200 (for lavage) or 1:400 (for serum) in assay buffer and kept on ice before use.

After wetting the wells of a MultiScreen HTS HV filter plate by adding 100 μ l assay buffer (PBS, pH 7.4, containing 1% BSA and 0.05% Tween-20) followed by centrifugation at $300 \times g$ at room temperature for 45 sec, we added 5,000 beads of each gYghJ and nYghJ to 50 μ l assay buffer and combined this with 50 μ l diluted serum or lavage samples in the filter plate. After 30 min incubation at room temperature on our microplate shaker, the beads were washed twice, as described for the wash steps for the bead-preparations in the previous section, with 200 μ l assay buffer. We subsequently incubated the beads on a shaker at room temperature for 30 min in 50 μ L secondary antibody, followed by two washes with 200 μ L assay buffer, and resuspension of the beads in 200 μ l assay buffer, followed by analysis on an LSR Fortessa flow cytometer (BD Life Sciences, Franklin Lakes, NJ).

Single beads were identified and gated by using forward and side light scatter readings. The single beads were then gated on fluorescence emission intensity at 700 nm to identify the bead population and, therefore, YghJ variant, and at 520 nm to measure of the amount of IgA bound to each of the beads. The median fluorescence intensity (MFI) for each protein, or bead population, was estimated by using FlowJo, version 10.4.2 (BD Life Sciences).

The estimated MFI for each protein in each assay was normalized by interpolating from standard curves that had been created by running the assay on a dilution series of a high-titre sample and setting the highest MFI reading to 10,000 arbitrary units (AUs).

The lavage samples may have different levels of IgA as a result of variations in antibody secretion during the intestinal lavage sample collection, and the amount of lavage fluid the volunteers consumed. To be able to compensate for different IgA levels in these samples, we measured the IgA concentration in all lavage samples by using the Human IgA Flex Set Kit (BD Life Sciences), as described by the producer. We then normalized the anti-YghJ assay results, measured in AUs, by dividing with the estimated total IgA concentration in the given sample to obtain normalized arbitrary units (nAUs).

Glycosylation specificity assay

To evaluate the degree to which anti-YghJ IgA responses specifically target glycosylated YghJ epitopes, we designed and performed a glycosylation specificity assay. In this assay, we pre-incubated the serum or lavage samples with non-glycosylated YghJ so that anti-YghJ antibodies that do not target glycosylated epitopes have been bound to free YghJ and, therefore, are hindered from reacting with bead-bound YghJ in the subsequent bead-based anti-YghJ antibody assay. By comparing the estimated anti-YghJ IgA levels in these samples with those of the untreated samples and of the samples that had been treated with glycosylated YghJ, we can calculate the proportion of the anti-YghJ IgA response that target epitopes specific for glycosylated YghJ. This is done by first subtracting the assay background (i.e., estimated antibody levels after pre-incubating the sample with glycosylated YghJ) from the antibody levels estimated from untreated and non-glycosylated YghJ-treated samples, followed by dividing the antibody levels estimated from non-glycosylated YghJ-treated samples with those of the untreated samples.

After diluting three parallels of the given sample, as described for the bead based anti-YghJ antibody assay, above (i.e., serum diluted 1:100 in assay buffer and lavage diluted 1:2 in 2X assay buffer), we added 1 µg nYghJ, 1 µg gYghJ, and 1 µL assay buffer, respectively, to the three parallels and incubated them shaken at room temperature for 30 min. The samples were then analysed in the bead based anti-YghJ antibody assay as described above. The 1 µg YghJ used in the pre-incubation step represents >300 times the quantity of YghJ bound to the beads that are added to the assays (calculations not shown).

Statistical Analysis

For all statistical analyses and for preparing graphs, we used Prism, version 9 (GraphPad Software, San Diego, CA), and we considered p-values ≤ 0.05 to be statistically significant. To test for differences in IgA levels between day-0 and day-10 serum and lavage samples, we used Wilcoxon signed-rank test. To test for differences in IgA levels between volunteers who developed diarrhoea and those who did not, we used the Mann-Whitney U test. To assess the correlation in IgA levels between and within lavage and serum samples we calculated Pearson correlation coefficients.

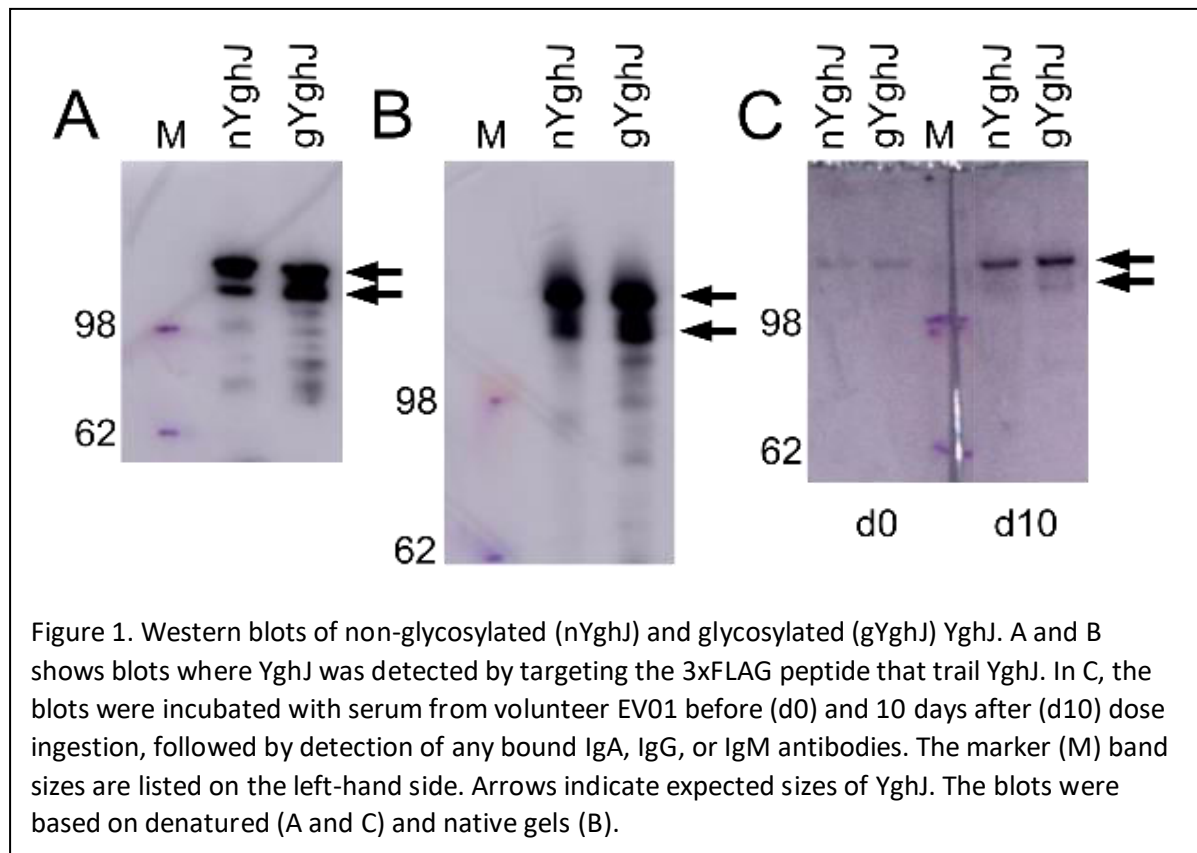
Ethical approval

All volunteers signed written informed consent to participate in the study and could leave at any point at their discretion. This project is registered under Helse Bergen and the experimental infection study (NCT02870751 at ClinicalTrials.gov) was approved by the Regional Committee for Medical and Health Research Ethics, Health Region West (REC-West; case number 2014/826).

RESULTS

Protein testing

We found that the non-glycosylated YghJ and the native, glycosylated YghJ had the expected sizes when separated by native and denaturing gel electrophoresis and detected by anti-FLAG



antibodies (Figure 1). This indicated no gross conformational differences between our non-glycosylated and glycosylated YghJ preparations.

To test whether the antibodies that volunteers developed could specifically targeted our purified YghJ, we tested serum from our first volunteer (EV01) against the purified proteins in a denaturing western blot. We found that serum collected immediately before dose ingestion contained antibodies that targeted a protein that had the same size as YghJ, and that the serum antibody levels had increased 10 days afterwards (Figure 1C), suggesting that our purified YghJ are recognized by anti-YghJ antibodies produced by the volunteers. There appeared to be no other strong bands in those blots, suggesting that the results of our bead assays will reflect antibody levels against YghJ and not against any other proteins potentially contaminating the protein preparations.

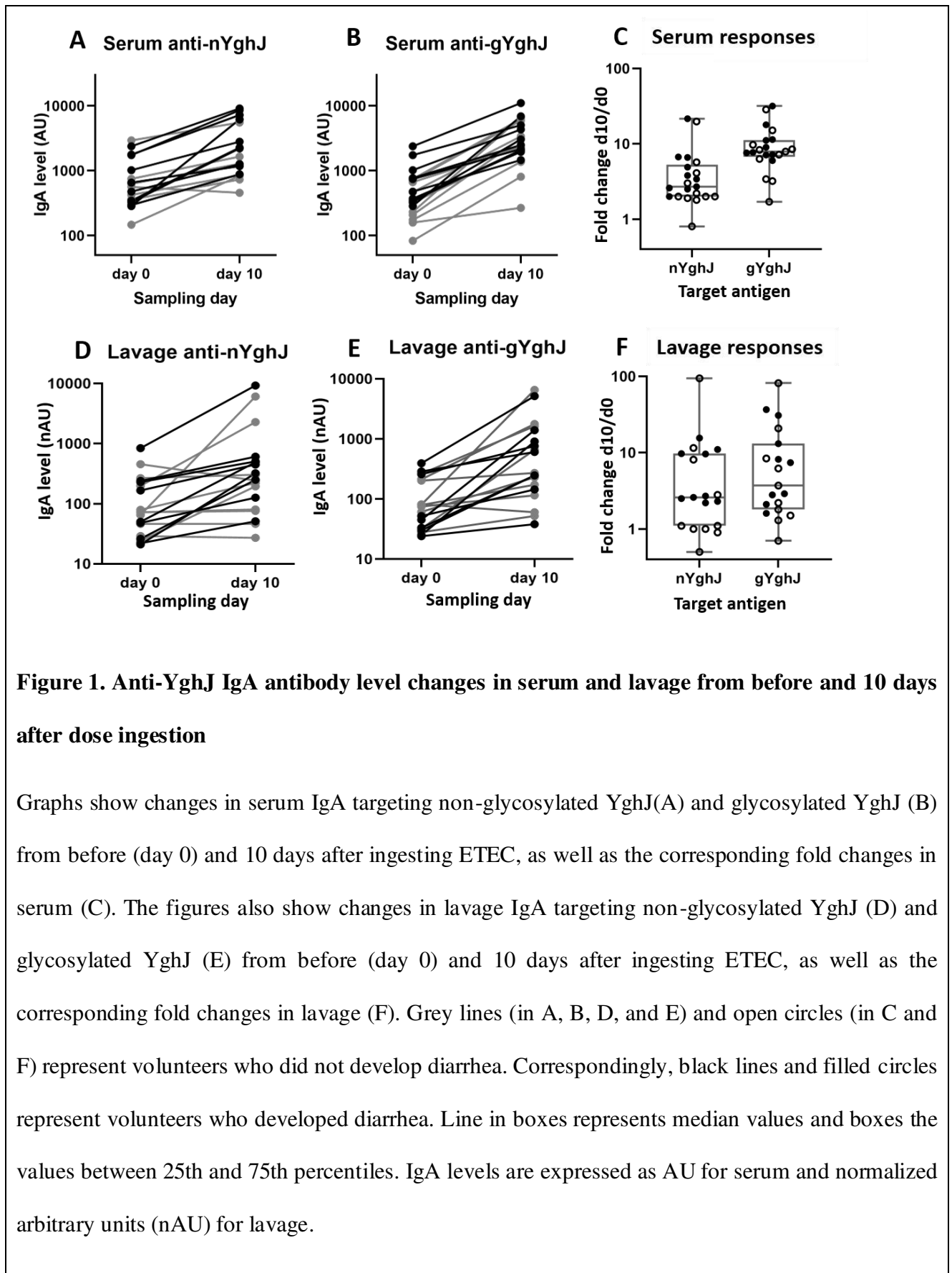
The BEMAP analyses showed that the purified glycosylated TW10722 YghJ is O-linked hyper-glycosylated, with 64 O-glycosylated serine and threonine residues. This is ten more positions than previously shown in the ETEC H10407 reference strain. A total of 34 glycosylation sites found in this analysis were not found in the ETEC reference strain (Thorsing et al., submitted for publication).

Serum and lavage samples

We included in the analysis a complete set of 21 serum and lavage samples taken before (day 0), and at 10 days (day 10) after the dose was ingested. Ten of the sample pairs were from volunteers who developed diarrhoea. Lavage samples from two volunteers were excluded because we could not detect any IgA in one of their two samples. Correspondingly, 19 pairs of lavage samples were included in the analyses. Median total IgA concentration in the lavage samples was 0.7 (IQR: 0.6, 1.9) mg/mL in the day 0 samples and 1.4 (IQR: 0.7, 2.2) mg/mL in the day 10 samples, with the difference not being statistically significant.

Changes in anti-YghJ IgA levels following ETEC infection

To evaluate the IgA antibody response to YghJ following the experimental infection, we estimated the change in levels of YghJ-specific IgA antibodies serum and lavage from day 0 to day 10.



We found that the anti-YghJ IgA levels in serum rose significantly from day 0 to day 10, both when tested against nYghJ (median 564 [IQR: 360, 770] AU on day 0 to 1653 [IQR: 1181, 5553] AU on day 10; $p < 0.001$; Figure 1A) and against gYghJ (median 299 [IQR: 208, 666] AU on day 0 to 2495 [IQR: 2042, 5042] AU on day 10; $p < 0.001$; Figure 1B). The corresponding median fold change was 2.7 (IQR: 2.0, 4.9) for nYghJ and 7.9 (IQR: 7.1, 11.1) for gYghJ (Figure 1C) with no statistically significant difference between the two variants. Defining responders to be volunteers who had ≥ 2.0 -fold increase in anti-YghJ IgA levels, we found that 18 of the 21 volunteers (86%) were responders when tested against nYghJ, while 20 of 21 (95%) were responders when tested against gYghJ.

Also for the lavage samples, we found significant increases in median anti-nYghJ IgA levels from day 0 to day 10, both when tested against nYghJ (median 72 [IQR: 37, 213] nAU on day 0 to 250 [IQR: 103, 497] nAU on day 10; $p = 0.007$; Figure 1D) and against gYghJ (median 75 [IQR: 32, 207] nAU on day 0 to 271 [IQR: 158, 1151] nAU on day 10; $p < 0.001$; Figure 1E). The corresponding median fold change was 2.6 (IQR: 1.1, 9.7) for nYghJ and 3.7 (IQR: 2.0, 10.7) for gYghJ (Figure 1F), with no statistically significant difference between the two variants. Thirteen of the 19 volunteers (68%) were responders when testing against nYghJ, while 14 of 19 (74%) were responders when testing against gYghJ. Neither in serum, nor in lavage, did we find any statistically significant difference in anti-YghJ IgA levels between volunteers who developed diarrhoea compared to those who did not.

Anti-nYghJ and anti-gYghJ IgA fold change responses correlated well in serum ($r = 0.92$, $p < 0.001$) as well as in lavage ($r = 0.90$, $p < 0.001$) (Supplementary figure 1). There was no significant correlation between estimated anti-YghJ IgA levels in serum and lavage samples ($r = 0.10$ for nYghJ; $p = 0.68$, and $r = 0.09$ for gYghJ; $p = 0.71$) (Supplementary figure 2).

Proportion of anti-YghJ IgA targeting glycosylated epitopes

Here we estimated the proportion of anti-YghJ IgA antibodies that target glycosylated epitopes on YghJ. To obtain accurate estimates, we focused these analyses on the day 10 samples and only on the samples that had anti-YghJ levels ≥ 100 AU (for serum) and ≥ 100 nAU (for lavage). We, therefore, included 16 serum and 11 lavage samples in these analyses.

We pre-incubated the samples with 1 μg of glycosylated or non-glycosylated YghJ before measuring the levels of anti-YghJ IgA that were still free to bind to the beads. We found that samples that had been pre-incubated with 1 μg glycosylated YghJ gave the same results as those that had jointly been pre-incubated with both glycosylated and non-glycosylated YghJ (data not shown), suggesting that our glycosylated YghJ presents all the epitopes also found on the non-glycosylated YghJ. We, therefore, used results from the glycosylated YghJ pre-incubation as measures of the assay background. To measure the fraction of anti-YghJ IgA that target glycosylated epitopes, we pre-incubated the samples with non-glycosylated YghJ and compared the results with those from samples that had not been pre-treated, after subtracting the assay background as explained in Methods and Materials.

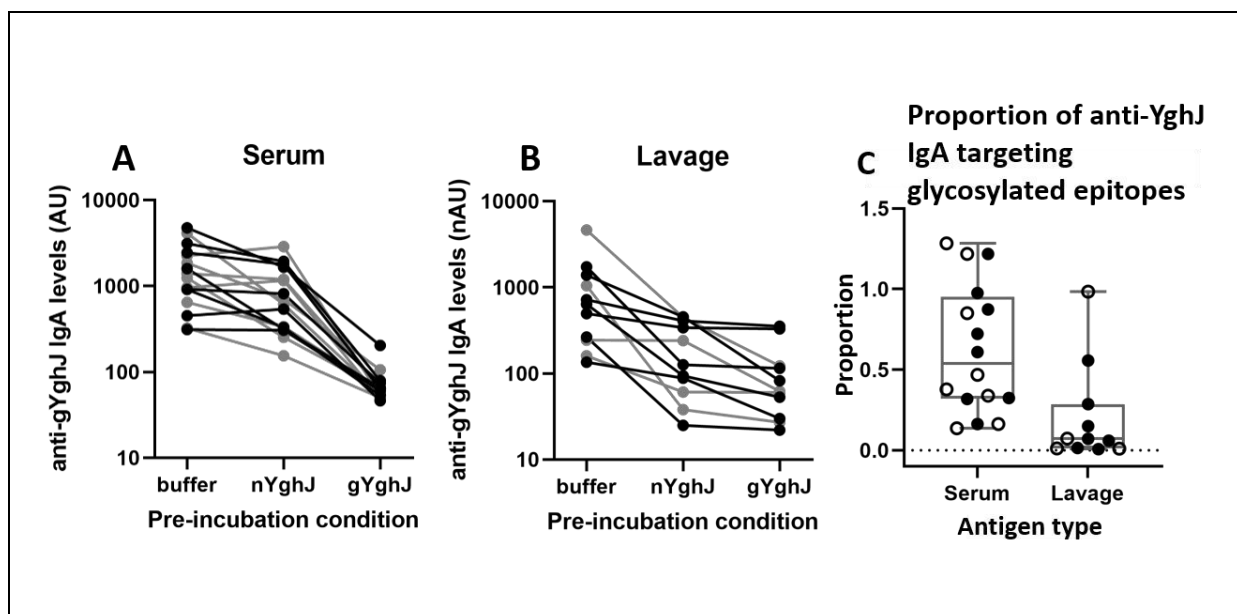
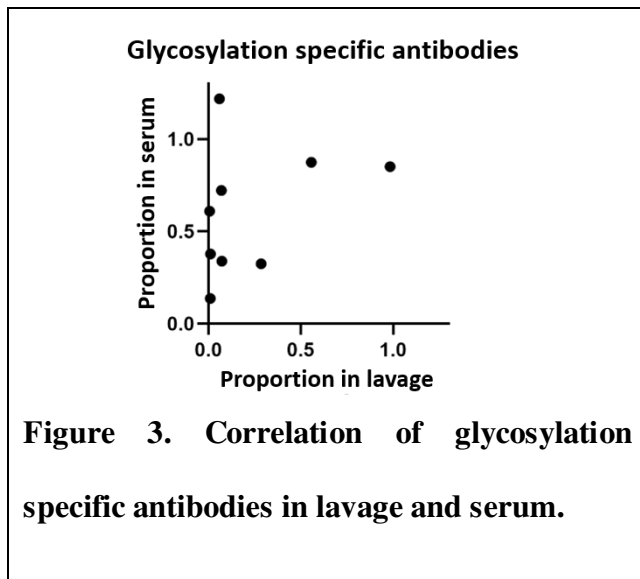


Figure 2. Glycosylated epitope specificity in serum and lavage.

Graphs show anti-gYghJ antibody levels in serum after pre-incubation with buffer or nYghJ, or gYghJ (A) and anti-gYghJ antibody levels in lavage after pre-incubation with buffer or nYghJ, or gYghJ (B). Graph C shows the proportion of anti-gYghJ-specific antibodies out of total anti-nYghJ and anti-gYghJ specific IgA antibodies in serum and lavage. Grey lines and open circles represent volunteers who did not develop diarrhea. Correspondingly, black lines and filled circles represent volunteers who developed diarrhea. Line in the boxes represents median values and boxes the values between 25th and 75th percentiles. The upper and lower whiskers limit 95% of measured values. IgA levels are expressed as AU for serum and normalized arbitrary units (nAU) for lavage.

In serum, the median anti-gYghJ IgA antibody level was 1316 (IQR: 844, 2301) AU (Figure 2A, "buffer" column), the median IgA level for antibodies targeting glycosylated YghJ epitopes was 656 (IQR: 326, 1310) AU (Figure 2A, column "nYghJ"), and the median assay background was 63 (IQR: 53, 68) AU (Figure 2A, column "gYghJ"). The median proportion of anti-YghJ IgA antibodies that target glycosylated epitopes in these 16 volunteers was consequently 0.54 (IQR: 0.32, 0.90) (Figure 2C, column "Serum").

In lavage, the median anti-gYghJ IgA antibody level was 638 (IQR: 254, 1,217) nAU (Figure 2B, "buffer" column), the median IgA level for antibodies targeting glycosylated YghJ epitopes was 126 (IQR: 74, 373) nAU (Figure 2B, "nYghJ" column), while the median assay background was 62 (IQR: 41, 119) nAU (figure 2B, "gYghJ" column). The median proportion of anti-YghJ IgA antibodies that target glycosylated epitopes in these 11 volunteers was consequently 0.07 (IQR: 0.01, 0.22) (Figure 2C, column "Lavage").



As seen in Figure 3, In the nine volunteers where data was available for both serum and lavage, there appeared to be little correlation between the estimated proportions of glycosylation-specific IgA between serum and lavage ($r = 0.35$, $p = 0.34$). Three of the volunteers showed substantial proportions of antibodies against glycosylated epitopes in both lavage and serum, while in the remaining six volunteers serum proportions were not reflected in lavage or were low in both.

DISCUSSION

We found that infection with ETEC TW10722 elicited strong IgA responses against YghJ in volunteers and that antibodies against both glycosylated and non-glycosylated versions of the protein could be consistently detected both in serum and lavage.

To study the antibody response that targets glycosylated epitopes on YghJ, we expressed the protein under its native promoter in TW10722 to ensure that the native level of protein modification was maintained. The results from our BEMAP analyses suggest that TW10722 heavily glycosylates YghJ. In a recently completed study, Thorsing *et al*; submitted) used BEMAP analyses on YghJ isolated from ETEC reference strain H10407 and found that it is

O-linked hyper-glycosylated, with 54 of the amino acid residues being glycosylated. In our analyses we found that 64 of the residues were glycosylated and approximately half of the sites being shared between the two ETEC strains. This indicates that considerable glycosylation of YghJ is likely to be common in ETEC, but that the glycosylation quantity and quality will vary between strains.

Some volunteers appeared to have high pre-existing levels of anti-YghJ IgA antibodies both in serum and in lavage, with day 0 levels that were 5- and 11-fold higher than the median in serum and lavage, respectively. Interestingly, it was these volunteers who also exhibited strong responses at day 10. Pre-existing immunity against YghJ may not be uncommon as both pathogenic and many commensal *E. coli* produce YghJ (30).

Given the nature of the lavage sample collection, where the volunteers needed to drink large quantities of laxatives, variation in antibody levels between different lavage samples is expected. The variation is caused by the differences in amount of liquid consumed, differences in intestinal peristalsis, or the presence of contaminants that increase background or neutralize antibodies. To compensate for this variation, we estimated the anti-YghJ IgA levels by using arbitrary units instead of MFI values, and we normalized the estimates by adjusting for the total IgA concentration in the lavage samples. Gut inflammation associated with infection may prompt bystander activation of B cells in GALT and increased production of polyclonal IgA antibodies (31). Although not significant, we did observe a rise in total IgA levels from day 0 to day 10. Normalizing against total IgA, therefore, has likely resulted in a conservative estimation of fold changes.

The finding that only 3 of 11 volunteers seemed to have any substantial proportion of IgA that targeted glycosylated epitopes is surprising, given that close to all of the volunteers had relatively high levels of IgA targeting glycosylated epitopes in their serum samples. We have

not been able to find any data in the literature regarding differential systemic and intestinal antibody specificities against glycosylated epitopes, but our finding is similar to findings of less anti-citrullinated protein IgA antibodies in saliva compared to serum in patients with rheumatoid arthritis (32).

Surprisingly, in some of the volunteers, pre-incubation of samples with nYghJ resulted in an anti-gYghJ antibody response that was higher than when the samples were pre-incubated with buffer only. For serum, this might be explained by depletion of all IgA, IgM, and IgG antibodies specific for nYghJ leading to more glycosylated epitopes being available for the remaining anti-gYghJ IgA antibodies to bind, leading to stronger secondary IgA signals than in the non-depleted samples. However, this explanation cannot be generalized to lavage, where IgG and IgM antibodies are expected to be negligible. However, higher variability of antibody levels in lavage may be the reason for inaccurate quantitation in this assay. Further studies are needed to decipher the observed difference between serum and lavage proportions.

Our study confirms the antigenicity of the ETEC mucinase YghJ in humans. We also provide evidence that natural ETEC infection with exposure to YghJ elicits an IgA antibody response, in both blood and the gut, with antibodies targeting not only the protein backbone epitopes, but also glycosylated epitopes. We found that the proportion of antibodies targeting the glycosylated epitopes varied greatly between individuals and that the proportion was considerably higher in IgA from the blood than from the gut. Further studies will be needed to elucidate the role of these glycosylation-specific antibodies in protecting against ETEC infection.

Conflict of interest

AB is listed as inventor on patent relating to WO 2017/059864 held by University of Southern Denmark and Aarhus University. AB and AZA have a financial interest in GlyProVac ApS, which has licensed exclusively the IP stated above. AB is the scientific founder, shareholder, and a member of the board. AZA is co-founder, shareholder, and a member of the board. AB, AZA and MT are employees of GlyProVac ApS. Other authors declare no conflict of interest.

Funding: This work was supported by the University of Bergen and Innovation Fund Denmark (Grant #7041-00220)

Author contribution statement

SR, HS, AZA, AB and KH conceived and designed the experiments. SR, HS, AB and KH wrote the first draft of the manuscript. SR, HS, AZA, AB and KH analyzed data. SR and KH performed the bead assay experiments. MT performed cloning and generated strains used for producing YghJ. AB produced the YghJ and analyzed the mass spectrometry data. All authors contributed to the manuscript and approved the submitted version.

Acknowledgements:

We thank Rikke Bækhus Jakobsen for performing the protein purification and PAGE experiments, and Arkadiusz Nawrocki for processing the mass spectrometry samples.

REFERENCES

1. Khalil IA, Troeger C, Blacker BF, Rao PC, Brown A, Atherly DE, et al. Morbidity and mortality due to shigella and enterotoxigenic *Escherichia coli* diarrhoea: the Global Burden of Disease Study 1990-2016. *Lancet Infect Dis*. 2018;18(11):1229-40.
2. Anderson JDt, Bagamian KH, Muhib F, Amaya MP, Laytner LA, Wierzba T, et al. Burden of enterotoxigenic *Escherichia coli* and shigella non-fatal diarrhoeal infections in 79 low-income and lower middle-income countries: a modelling analysis. *Lancet Glob Health*. 2019;7(3):e321-e30.
3. Levine MM, Barry EM, Chen WH. A roadmap for enterotoxigenic *Escherichia coli* vaccine development based on volunteer challenge studies. *Hum Vaccin Immunother*. 2019;15(6):1357-78.
4. Mirhoseini A, Amani J, Nazarian S. Review on pathogenicity mechanism of enterotoxigenic *Escherichia coli* and vaccines against it. *Microb Pathog*. 2018;117:162-9.
5. Chakraborty S, Randall A, Vickers TJ, Molina D, Harro CD, DeNearing B, et al. Interrogation of a live-attenuated enterotoxigenic *Escherichia coli* vaccine highlights features unique to wild-type infection. *NPJ Vaccines*. 2019;4:37.
6. Luo Q, Qadri F, Kansal R, Rasko DA, Sheikh A, Fleckenstein JM. Conservation and immunogenicity of novel antigens in diverse isolates of enterotoxigenic *Escherichia coli*. *PLoS Negl Trop Dis*. 2015;9(1):e0003446.
7. Tapader R, Bose D, Pal A. YghJ, the secreted metalloprotease of pathogenic *E. coli* induces hemorrhagic fluid accumulation in mouse ileal loop. *Microb Pathog*. 2017;105:96-9.
8. Luo Q, Kumar P, Vickers TJ, Sheikh A, Lewis WG, Rasko DA, et al. Enterotoxigenic *Escherichia coli* secretes a highly conserved mucin-degrading metalloprotease to effectively engage intestinal epithelial cells. *Infect Immun*. 2014;82(2):509-21.
9. Strozen TG, Li G, Howard SP. YghG (GspS β) Is a Novel Pilot Protein Required for Localization of the GspS Type II Secretion System Secretin of Enterotoxigenic *Escherichia coli*. *Infection and Immunity*. 2012;80(8):2608-22.
10. Yang J, Baldi DL, Tauschek M, Strugnelli RA, Robins-Browne RM. Transcriptional Regulation of the yghJ-pppA-yghG-gspCDEFGHIJKLM Cluster, Encoding the Type II Secretion Pathway in Enterotoxigenic *Escherichia coli*. *Journal of Bacteriology*. 2007;189(1):142-50.
11. Nesta B, Valeri M, Spagnuolo A, Rosini R, Mora M, Donato P, et al. SsIE elicits functional antibodies that impair in vitro mucinase activity and in vivo colonization by both intestinal and extraintestinal *Escherichia coli* strains. *PLoS Pathog*. 2014;10(5):e1004124.
12. Todnem Sakkestad S, Steinsland H, Skrede S, Kleppa E, Lillebo K, Saevik M, et al. Experimental Infection of Human Volunteers with the Heat-Stable Enterotoxin-Producing Enterotoxigenic *Escherichia coli* Strain TW11681. *Pathogens*. 2019;8(2).
13. Sakkestad ST, Steinsland H, Skrede S, Lillebo K, Skutlaberg DH, Guttormsen AB, et al. A new human challenge model for testing heat-stable toxin-based vaccine candidates for enterotoxigenic *Escherichia coli* diarrhea - dose optimization, clinical outcomes, and CD4+ T cell responses. *PLoS Negl Trop Dis*. 2019;13(10):e0007823.
14. Chakraborty S, Randall A, Vickers TJ, Molina D, Harro CD, DeNearing B, et al. Human Experimental Challenge With Enterotoxigenic *Escherichia coli* Elicits Immune Responses to Canonical and Novel Antigens Relevant to Vaccine Development. *J Infect Dis*. 2018;218(9):1436-46.
15. .
16. Fleckenstein JM, Roy K, Fischer JF, Burkitt M. Identification of a two-partner secretion locus of enterotoxigenic *Escherichia coli*. *Infect Immun*. 2006;74(4):2245-58.

17. Knudsen SK, Stensballe A, Franzmann M, Westergaard UB, Otzen DE. Effect of glycosylation on the extracellular domain of the Ag43 bacterial autotransporter: enhanced stability and reduced cellular aggregation. *Biochem J.* 2008;412(3):563-77.
18. Lindenthal C, Elsinghorst EA. Identification of a glycoprotein produced by enterotoxigenic *Escherichia coli*. *Infect Immun.* 1999;67(8):4084-91.
19. Lindenthal C, Elsinghorst EA. Enterotoxigenic *Escherichia coli* TibA glycoprotein adheres to human intestine epithelial cells. *Infect Immun.* 2001;69(1):52-7.
20. Boysen A, Palmisano G, Krogh TJ, Duggin IG, Larsen MR, Moller-Jensen J. A novel mass spectrometric strategy "BEMAP" reveals Extensive O-linked protein glycosylation in Enterotoxigenic *Escherichia coli*. *Sci Rep.* 2016;6:32016.
21. Lisowska E. The role of glycosylation in protein antigenic properties. *Cell Mol Life Sci.* 2002;59(3):445-55.
22. Lithgow KV, Scott NE, Iwashkiw JA, Thomson EL, Foster LJ, Feldman MF, et al. A general protein O-glycosylation system within the Burkholderia cepacia complex is involved in motility and virulence. *Mol Microbiol.* 2014;92(1):116-37.
23. Wolfert MA, Boons GJ. Adaptive immune activation: glycosylation does matter. *Nat Chem Biol.* 2013;9(12):776-84.
24. Wang S, Voronin Y, Zhao P, Ishihara M, Mehta N, Porterfield M, et al. Glycan Profiles of gp120 Protein Vaccines from Four Major HIV-1 Subtypes Produced from Different Host Cell Lines under Non-GMP or GMP Conditions. *J Virol.* 2020;94(7).
25. Romain F, Horn C, Pescher P, Namane A, Riviere M, Puzo G, et al. Deglycosylation of the 45/47-kilodalton antigen complex of *Mycobacterium tuberculosis* decreases its capacity to elicit in vivo or in vitro cellular immune responses. *Infect Immun.* 1999;67(11):5567-72.
26. Uzzau S, Figueroa-Bossi N, Rubino S, Bossi L. Epitope tagging of chromosomal genes in *Salmonella*. *Proc Natl Acad Sci U S A.* 2001;98(26):15264-9.
27. Boysen A, Moller-Jensen J, Kallipolitis B, Valentin-Hansen P, Overgaard M. Translational regulation of gene expression by an anaerobically induced small non-coding RNA in *Escherichia coli*. *J Biol Chem.* 2010;285(14):10690-702.
28. Maigaard Hermansen GM, Boysen A, Krogh TJ, Nawrocki A, Jelsbak L, Moller-Jensen J. HldE Is Important for Virulence Phenotypes in Enterotoxigenic *Escherichia coli*. *Front Cell Infect Microbiol.* 2018;8:253.
29. Urban JH, Vogel J. Translational control and target recognition by *Escherichia coli* small RNAs in vivo. *Nucleic Acids Res.* 2007;35(3):1018-37.
30. Moriel DG, Bertoldi I, Spagnuolo A, Marchi S, Rosini R, Nesta B, et al. Identification of protective and broadly conserved vaccine antigens from the genome of extraintestinal pathogenic *Escherichia coli*. *Proc Natl Acad Sci U S A.* 2010;107(20):9072-7.
31. Aase A, Sommerfelt H, Petersen LB, Bolstad M, Cox RJ, Langeland N, et al. Salivary IgA from the sublingual compartment as a novel noninvasive proxy for intestinal immune induction. *Mucosal Immunology.* 2016;9(4):884-93.
32. Roos Ljungberg K, Borjesson E, Martinsson K, Wettero J, Kastbom A, Svard A. Presence of salivary IgA anti-citrullinated protein antibodies associate with higher disease activity in patients with rheumatoid arthritis. *Arthritis Res Ther.* 2020;22(1):274.

Supplementary information

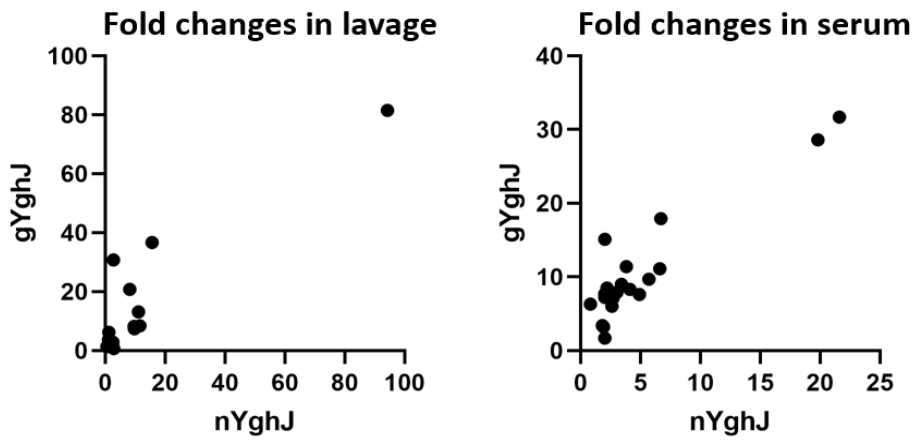
Supplementary table S1: Strains, plasmids and cell lines used in this study.

Strains	Genotype	Antibiotic resistance	Reference
ETEC TW10722			(1)
<i>E. coli</i> Top10	F- <i>mcrA</i> Δ (<i>mrr-hsdRMS-mcrBC</i>) ϕ 80 <i>lacZ</i> Δ M15 Δ <i>lacX74 nupG</i> <i>recA1 araD139</i> Δ (<i>ara-leu</i>)7697 <i>galE15 galK16 rpsL</i> (StrR) <i>endA1</i> λ - . Used for cloning		Invitrogen
MG1655 Δ <i>hldE</i>	<i>hldE</i> isogenic knockout strain		(2)
TW10722 <i>yghJ</i>	3xFLAG epitope tagging of <i>yghJ</i> on chromosome		This study
Plasmids			
pKD46	Red recombinase expression vector. Temperature sensitive – replicates at 30C	Amp ^R	(3)
pSUB11	Used for 3xFLAG epitope tagging on chromosome	Kan ^R	(4)
pXG-0	Low copy number plasmid	Cml ^R	(5)
pGPV106	Plasmid used for overexpression of ETEC TW10722 <i>yghJ</i> 3xFLAG	Cml ^R	This study

References to table 1.

1. Sakkestad ST, Steinsland H, Skrede S, Lillebo K, Skutlaberg DH, Guttormsen AB, et al. A new human challenge model for testing heat-stable toxin-based vaccine candidates for enterotoxigenic *Escherichia coli* diarrhea - dose optimization, clinical outcomes, and CD4+ T cell responses. *PLoS Negl Trop Dis*. 2019;13(10):e0007823.
2. Maigaard Hermansen GM, Boysen A, Krogh TJ, Nawrocki A, Jelsbak L, Moller-Jensen J. HldE Is Important for Virulence Phenotypes in Enterotoxigenic *Escherichia coli*. *Front Cell Infect Microbiol*. 2018;8:253.
3. Datsenko KA, Wanner BL. One-step inactivation of chromosomal genes in *Escherichia coli* K-12 using PCR products. *Proceedings of the National Academy of Sciences of the United States of America*. 2000;97(12):6640-5.
4. Uzzau S, Figueroa-Bossi N, Rubino S, Bossi L. Epitope tagging of chromosomal genes in *Salmonella*. *Proc Natl Acad Sci U S A*. 2001;98(26):15264-9.
5. Urban JH, Vogel J. Translational control and target recognition by *Escherichia coli* small RNAs in vivo. *Nucleic Acids Res*. 2007;35(3):1018-37.

Supplementary figure 1. Correlation between lavage and serum fold changes for anti-nYghJ and anti-gYghJ antibodies.



Supplementary figure 2. Correlation between nYghJ and gYghJ fold changes in lavage and in serum.

